Guo *et al. Ecological Processes* (2026) 15:42
https://doi.org/10.1186/s13717-026-00700-w

Ecological Processes

RESEARCH **Open Access**

Elemental-enzymatic indicators of nutrient limitation in ombrotrophic peatlands across seasonal and spatial gradients

Shuaizhi Guo[1*], Danny Turner[1], Deying Wang[1], Donald T. Monteith[2], Niall P. McNamara[2], Gary D. Bending[1] and Ryan M. Mushinski[1*]

Abstract

Background Blanket bogs are rare ombrotrophic peatlands that function as important long-term carbon stores. Their persistence depends on strong nutrient limitation, which maintains *Sphagnum* dominance and suppresses decomposition, yet mechanisms driving seasonal and spatial variability in microbial nitrogen and phosphorus limitation patterns remain poorly understood. This study investigated nutrient soil limitation dynamics by integrating plant elemental stoichiometry with microbial enzymatic stoichiometry.

Results We conducted snapshot sampling during two contrasting seasons (summer 2023 and winter 2024) along an elevational sequence (550–750 m) and across peat depths (0–60 cm). Given the high-water content of peat soils (~86% moisture), we focused on enzyme stoichiometric ratios rather than absolute enzyme activities, specifically the ratio of urease to acid phosphatase. Seasonal variation dominated patterns in both soil elemental stoichiometry and microbial enzymatic stoichiometry. Depth gradients were equally strong, with N:P increasing down-profile. This highlights rapid seasonal reorganisation at the surface versus slower, depth-driven changes from peat development. Soil nitrogen-to-phosphorus ratios were tightly coupled to microbial enzyme stoichiometry, following an inverse power-law relationship (exponent $= -1.56$, $R^2 = 0.60$). From this relationship, we derived a urease-based microbial nitrogen acquisition threshold (urease:acid phosphatase = 88; 95% confidence interval: 64–118), which showed strong correspondence with the canonical plant nitrogen-to-phosphorus limitation threshold of 16, used here as a reference for ecosystem-level nutrient balance. Microbial community composition corroborated these patterns, with bacterial-to-fungal ratios 4.3-fold higher in winter than summer (18.9-fold in surface peat), consistent with observed N:P stoichiometric gradients, suggesting that seasonal changes in microbial community structure align with variation in nutrient availability, while also reflecting the influence of additional environmental controls.

Conclusions Our findings demonstrate a strong coupling between plant–soil nutrient stoichiometry and microbial enzyme allocation in blanket bogs, structured by the interaction of dynamic seasonal forcing and persistent depth-related constraits. Seasonal processes regulate short-term nutrient availability and microbial function in surface peat, whereas depth reflects long-term peat development that constrains the baseline stoichiometric framework of the system. Winter conditions were characterised by stoichiometric patterns consistent with relative N limitation at the ecosystem level, whereas summer conditions reflected stronger P constraint. We identified a quantitative microbial

---

*Correspondence:
Shuaizhi Guo
Shuaizhi.Guo@warwick.ac.uk
Ryan M. Mushinski
Ryan.Mushinski@warwick.ac.uk
Full list of author information is available at the end of the article

enzyme threshold that aligns with plant-derived nutrient limitation thresholds, directly linking microbial processes to ecosystem nutrient status and providing a robust framework for diagnosing nutrient limitation in water-saturated peat soils. Incorporating seasonal nutrient dynamics into peatland management may be critical for maintaining microbial functioning, vegetation structure, and long-term carbon sequestration.

Keywords Blanket bog, Enzymatic stoichiometry, Nitrogen limitation, Phosphorus limitation, Peatland biogeochemistry, Seasonal dynamics, Urease-phosphatase ratio

Background

Peatland ecosystems, characterised by waterlogged, anoxic, and acidic conditions, play a vital role in maintaining biodiversity, regulating water quality, reducing flood risk, and mitigating climate change (Evans et al. 2016; Ritson et al. 2025). In the United Kingdom, peatlands cover approximately 12% of the land area, with blanket bogs as the most widespread type; yet these represent the rarest form of ombrotrophic peatland globally (Swinnen et al. 2019). Blanket bogs typically develop under high rainfall (> 1,000 mm yr^{-1}) and low temperature (< 15 °C) regimes (Lindsay et al. 1988). They occur predominantly on flat to gently sloping uplands from sea level to elevations above 1,000 m (Natural England 2015) and can reach depths from a few centimetres to several metres (Lindsay 1995). Their extensive distribution creates substantial spatial heterogeneity in peat biogeochemistry. Seasonal fluctuations in temperature, precipitation, and water-table level further shape the biotic and abiotic dynamics of ombrotrophic peatlands, driving shifts in land condition, peat shrinkage, elemental storage and greenhouse-gas emission (Armstrong et al. 2015; Morton and Heinemeyer 2019; Feng et al. 2020; Evans et al. 2021). These ecosystems are highly vulnerable, with even minor environmental disturbances able to disrupt their balance and alter ecosystem functioning (Lunt et al. 2019; Ferretto et al. 2019; UNEP 2022). This heterogeneity limits the validity of spatially limited peatland studies, underscoring the need to quantify the relative importance of seasonal versus spatial factors in driving peatland biogeochemical processes.

Globally, peatlands store ~ 450–650 Gt carbon (C), accounting for roughly 25% of total soil C (UNEP 2022; Yin et al. 2022; Vesala et al. 2021), and they also serve as important long-term sinks for nitrogen (N) and phosphorus (P) (Arsenault et al. 2018). In ombrotrophic bogs, the term *ombrotrophic* refers to rain-fed hydrology rather than nutrient sources. Contemporary new inputs of N come from atmospheric deposition and biological N_2 fixation, while new P inputs come primarily from atmospheric deposition (Vile et al. 2014; Knorr et al. 2015). However, the majority of N and P cycling occurs through internal recycling of organic matter accumulated over millennia (Bünemann et al. 2011). The peat profile also contains legacy P derived from both historical atmospheric deposition and weathering of mineral substrates during peat development, with the relative contributions varying by site geology and peat age (Schillereff et al. 2021). These nutrients strongly regulate primary production and decomposition of the ecosystem (Schlesinger and Bernhardt 2020; Wang and Moore 2014). Consequently, the contents and stoichiometric ratios of C, N, and P act as key indicators of plant nutrient strategies and environmental nutrient limitation patterns. These ratios are well-established as proxies to infer ecosystem responses to environmental change (Elser et al. 2000; Güsewell 2004; Cao et al. 2020). However, the spatial and seasonal variability of elemental stoichiometric ratios, and the relative importance of their environmental drivers, remain poorly characterised in bog ecosystems. This limits our capacity to predict how peatland nutrient cycling will respond to environmental change.

Building on the Redfield concept, an N:P threshold of 16 has long served as a benchmark for N versus P limitation (Ptacnik et al. 2010; Gruber and Deutsch 2014). While this framework has been successfully applied to bryophytes (Bragazza et al. 2004; Jiroušek et al. 2011; Larmola et al. 2013) and vascular plants (Güsewell and Koerselman 2002; Olde Venterink et al. 2003), its application to bulk soil or peat stoichiometry requires careful conceptual consideration. Unlike plant tissue measurements, bulk peat represents an integrated and heterogeneous pool comprising accumulated plant litter, living and dead microbial biomass, partially decomposed and humified organic matter, and legacy nutrient pools that have developed over decadal to millennial timescales (Belyea and Malmer 2004; Wang et al. 2015; Tfaily et al. 2014). These components are continuously transformed through decomposition, microbial turnover, and internal nutrient recycling, resulting in stoichiometric signatures that reflect long-term ecosystem processes rather than instantaneous biological demand. Consequently, peat N:P ratios are more appropriately interpreted as indicators of ecosystem-level nutrient balance, integrating both contemporary biotic activity and historical accumulation processes, rather than as direct proxies for plant physiological nutrient limitation. Although bulk peat or soil stoichiometry can correlate with vegetation nutrient status under certain conditions (Wang and Moore 2014), this relationship is not necessarily one-to-one and may vary across environmental gradients. In particular, partial decoupling between peat and plant stoichiometry is expected in deeper peat horizons, where long-term diagenetic processes, selective P depletion, and reduced biological activity increasingly dominate the stoichiometric signal (Moore et al. 2018; Steinweg et al. 2018). Within this context, interpreting peat N:P ratios as ecosystem-level indicators provides a more appropriate framework for linking nutrient availability to both plant and microbial processes. This perspective is particularly relevant in ombrotrophic peatlands, where nutrient inputs are limited and internal recycling dominates biogeochemical dynamics.

Because microbes are central to organic matter turnover and nutrient release, their functional responses are critical for interpreting ecosystem-level stoichiometric patterns (Osburn et al. 2023). The C, N and P limitation of microbial activity has been documented across multiple ecosystems (Cui et al. 2025, 2022; Xu et al. 2022; Zhang et al. 2023). Soil enzyme stoichiometry has thus emerged as a powerful indicator of microbial nutrient limitation (Sinsabaugh et al. 2009). Fluorescein diacetate (FDA) hydrolysis is widely used to assess total microbial activity, reflecting the potential of the soil community to produce hydrolytic enzymes (Adam and Duncan 2001; Prosser et al. 2011). Among specific enzymes, urease (UA) catalyses the hydrolysis of urea to ammonia and CO_2, driving N mineralisation and accelerating organic N turnover, which can result in N losses (Motasim et al. 2024). Acid phosphatase (ACP), critical for P mobilisation in acidic peat soils, hydrolyses organic P into plant-available forms (Nannipieri et al. 2011). The UA:ACP ratio therefore provides a functional proxy of microbial preference for N versus P acquisition, directly linking enzymatic processes to nutrient limitation status. Although plant and microbial nutrient limitation are often decoupled due to intense competition for scarce N and P pools (Cui et al. 2021), recent global synthesis suggests that their nutrient constraints can align synergistically under certain environmental contexts (Xu et al. 2024). However, the response of enzyme stoichiometric ratios to nutrient limitation in blanket bog ecosystems remains poorly understood.

The use of enzyme activity ratios to infer nutrient limitation (ecoenzymatic stoichiometry) has been critiqued for oversimplifying microbial nutrient constraints (Mori 2020; Mori et al. 2023). Valid concerns include multiple enzymes can acquire the same nutrient, single enzymes can acquire multiple nutrients, and enzyme ratios may not reflect actual growth limitation (Rosinger et al. 2019). These critiques primarily address C:N:P frameworks using β-glucosidase, N-acetyl-β-glucosaminidase, and phosphatase ratios to infer C, N, and P co-limitation. However, N:P-focused enzyme ratios may be more robust than broader C:N:P frameworks. UA and ACP are relatively specific to N and P acquisition pathways, unlike β-glucosidase which can also support N acquisition via chitin degradation (Mori et al. 2021). Additionally, in nutrient-poor systems like ombrotrophic bogs where organic C is abundant, but N and P are scarce, microbial enzyme allocation is governed by relative N versus P scarcity rather than absolute C availability. Finally, we can validate N- and P-related enzyme ratios against independent measures of nutrient status (porewater chemistry, elemental stoichiometry) rather than using them as stand-alone indicators.

This study aimed to elucidate the mechanisms underlying nutrient limitation in ombrotrophic blanket bogs by integrating peat elemental stoichiometry with microbial enzymatic stoichiometry. Specifically, we sought to (1) Quantify the relative importance of seasonal versus spatial factors (elevation, depth) in driving elemental and enzymatic stoichiometries, and to characterise how these factors interact to shape peat physical properties, nutrient contents, and microbial biomass; (2) Establish the mechanistic coupling between elemental (N:P) and enzymatic (UA:ACP) stoichiometries; and (3) Characterise seasonal nutrient limitation at both plant and microbial levels, and assess its implications for the stability and functioning of blanket bog ecosystems.

Methods

Site description and soil sampling

The study was conducted at the Moor House National Nature Reserve, located in the Northern Pennines of England (54°41'N, 2°27'W). The climate of Moor House is classified as sub-Arctic oceanic. Summers are cool and wet, with July as the warmest month, exhibiting an average maximum temperature of 12.3 °C. Winters are cold and snowy, with temperatures averaging 1.2 °C in January, the coldest month (Supplementary Table S1). The site received an average annual precipitation of 1,633 mm between 2015 and 2023. The wettest months typically occur in November, December, and January, with an average monthly precipitation of 232 mm, while April, May and June are generally the driest, averaging 104 mm (Supplementary Figure S1). Sampling was conducted in July 2023 and February 2024 to represent summer and winter conditions, respectively. Sampling dates represented contrasting seasonal hydro-thermal conditions relative to recent climate records (Hollis et al. 2025). For the region of Northern England, July 2023 was cooler (15.2 °C, 20th percentile) and substantially wetter (157.1 mm, 178% of average) than typical summer conditions, while February

2024 was the warmest February on record for this period (6.6 °C, 1.78 °C above average) with above-average precipitation (105.5 mm, 115% of average). Regardless, these dates captured meaningful climate extremes, a cool, wet summer and an anomalously warm, wet winter. While this design does not capture intra-seasonal variability or interannual climate variation, it provides proof-of-concept for our hypothesised elemental-enzymatic coupling framework under contrasting hydro-thermal regimes.

The diverse habitats of the area include exposed summits, blanket peatlands, upland grasslands and pastures. The specific site of this work was the gently sloping eastern flank of Great Dun Fell, characterised by poorly drained glacial till that fosters the development of extensive blanket bog with peat depths ranging from 1 to 3 m (Supplementary Figure S2). The peat soils at Moor House are classified as Histosols under the World Reference Base for Soil Resources (IUSS Working Group WRB 2015), specifically Fibric Histosols in surface horizons (0–20 cm) with high fibric material content, transitioning to Hemic Histosols at depth (20–60 cm) with increasing humification. Under the UK national classification (Avery 1990), these correspond to raw peat soils of the Winter Hill association, characterised by ombrotrophic blanket peat developed on poorly drained upland terrain. More detailed information regarding the climate, vegetation, and environmental variables of the Moor House area can be accessed through the UK Environmental Change Network (ECN; www.ecn.ac.uk).

Samples were collected along a single elevational transect spanning five elevational bands (550 m, 600 m, 650 m, 700 m, 750 m; 50 m intervals) across 200 m of vertical relief on the eastern flank of Great Dun Fell (Fig. 1D). At each elevation, four replicate peat cores were extracted with horizontal spacing of approximately 100 m between replicates to capture local ecosystem variability, yielding 20 cores per sampling campaign (5 elevations × 4 replicates). Each core was divided into three depth layers (0–20 cm, 20–40 cm, 40–60 cm), producing 60 samples per season (20 cores × 3 depths) and 120 samples total across both seasons. This 200 m elevational range represents a temperature difference of approximately 1.3 °C

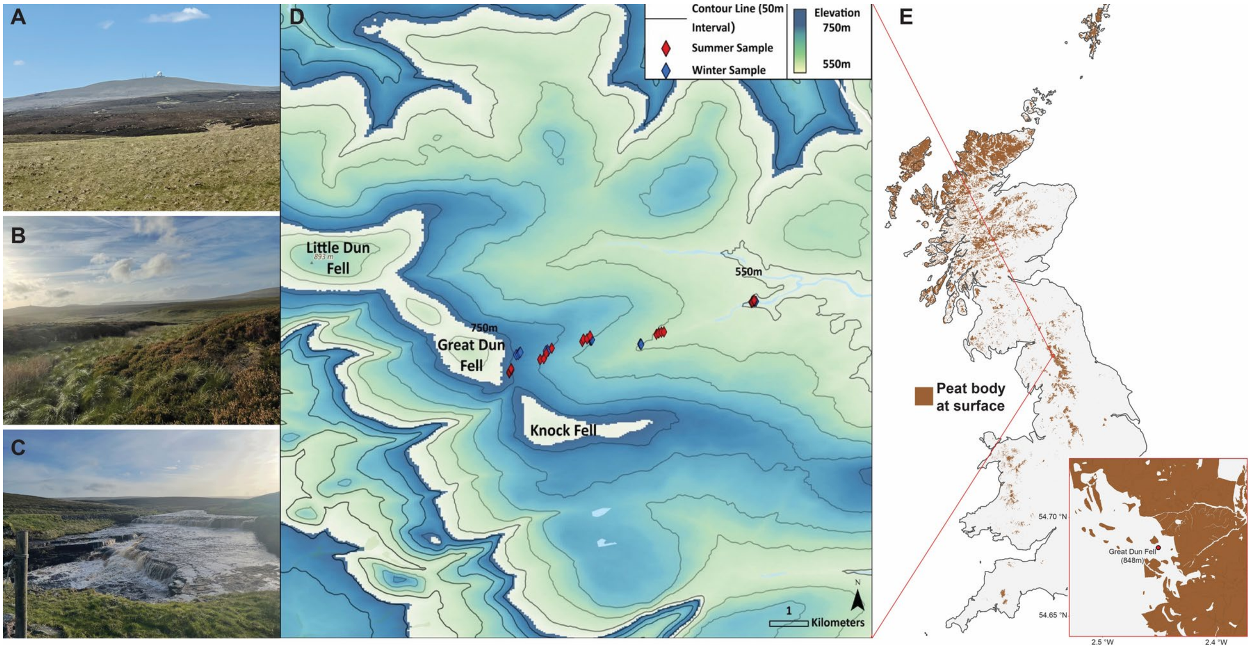

Fig. 1 Photos and maps of the Moor House study site. **A** Photo from the base of the sampling transect, facing upwards to the Great Dun Fell Radar Station. **B** Photo of the Moorhouse landscape taken at 650 m. **C** Photo of the stream Trout Beck which is adjacent to the lowest sampling points at 550 m. **D** Summer and winter sampling locations at Moor House National Nature Reserve, northern England. The topographic map shows the sampling transect from Great Dun Fell (highest) to the stream Trout Beck (lowest). The sampling design consisted of five elevational bands along a single transect on the eastern flank of Great Dun Fell, with four replicate cores collected at each elevation (individual sampling locations not shown at this map scale). Data from UKCEH Land Cover Map 2024 (Rowland et al. 2025). **E** Spatial distribution of peat coverage across Great Britain, showing peat bodies at the surface compiledfrom national inventories. Data sources include the NatureScot Carbon and Peatland Map 2016 (Scotland, *n* = 7,965 polygons), Natural England Priority Habitat Inventory (England, *n* = 22,251polygons), and the Natural Resources Wales Peatlands Map (Wales, *n* = 1 multipolygon). Brown shadingindicates mapped peatland extent. Map uses WGS84 coordinate system. Insert shows magnified depiction of peat coverage in the study area with Great Dun Fell as the central point

based on typical UK lapse rates (0.65 °C per 100 m; Burt and Holden 2010), providing modest environmental variation for assessing spatial effects relative to seasonal forcing. While the site's peat deposits extend to 1–3 m depth, we focused our analysis on the upper 60 cm, where seasonal signals are most pronounced and the majority of contemporary biogeochemical cycling occurs. At each elevation, four replicate peat samples, up to a depth of 60 cm, were extracted using a Russian peat corer and subsequentially divided into three layers: 0–20 cm, 20–40 cm, and 40–60 cm. Replicates were collected at each elevation for both seasons, with horizontal intervals of approximately 100 m between replicates, to account for local ecosystem variability. Sampling was completed over two days on each campaign. During the process, samples were packed in sterile Nasco Whirl–Pak™ giant-size sample bags and stored in a cold box filled with ice packs. They were then immediately transported to the laboratory, stored at 4 °C, and processed within seven days of collection.

Determination of peat physicochemical properties

Temperature and EC were measured on site using an RS PRO RS 1720 wired digital thermometer and Hanna GroLine direct soil EC tester with automatic temperature compensation, respectively. Both Probes were inserted approximately 5 cm horizontally into the side of each depth subsection immediately after core extraction, and readings were recorded once they stabilised. Peat pH was determined in extracts of 10 g of field-moist soil with 25 ml of deionised water by a pH meter (Mettler FiveEasy F20 pH/mV Meter). Moisture content was calculated by weighing 10 g of peat before and after oven drying at 60 °C for 48 h. Inorganic nutrients were extracted from 4 g homogenised subsamples of each soil sample using 20 ml of 0.01 M $CaCl_2$. Inorganic N assays were then conducted using a continuous segmented flow analyser (Seal Analytical, Ltd., U.K.) in accordance with ISO 13395 (nitrate + nitrite) and ISO 11732 (ammonium). PO_4^{3-} was analysed by the molybdate blue colorimetric method of Murphy and Riley (1962). Elemental analysis was performed using the precisION system in CNS mode, where 5 mg oven-dried and ground peat samples were combusted in an oxygen-rich environment, converting TC and TN into their gaseous forms, followed by separation via gas chromatography and quantification with a thermal conductivity detector (TCD). TP was determined using a modified nitric-peroxide block digestion (EPA Method 3050B), where 100 mg of oven-dried soil was digested with concentrated nitric acid at 120 °C for 10 h, followed by colorimetric measurement using the Murphy-Riley method.

qPCR analysis of soil microbiomes

Peat subsamples (0.25 g) were stored at − 20 °C and DNA was extracted within two days of sampling using the Qiagen DNeasy PowerSoil Kit. Extracted DNA was then stored at − 80 °C until quantitative real-time polymerase chain reaction (qPCR) analysis. DNA concentrations were quantified using the Qubit assay and standardised to 1 μg/ml for downstream analysis. The absolute abundances of the main groups comprising the microbiome (bacteria, archaea, fungi) were quantified using qPCR on an Agilent Technologies Stratagene Mx3005p system. Quantification was performed using an internal standard calibration curve with DNA standards for each target gene, ranging from 10^1 to 10^{10} copies. Each 10 μl reactant contained 5 μl of FastStart SYBR Green Master (Merck Ltd.), 3 μl of PCR-grade water, 1 μl of 10 μM primers, and 1 μl of DNA template. Product specificity was confirmed by observing a single peak in the melting curve, appearing between 80 °C and 90 °C. R^2 values for the standard curves and the estimated amplification efficiencies ranged between 0.91 and 1.07. Standards, negative controls and samples were run in duplicate. Copy numbers for each sample were calculated as the average of two analytical replicates. Information on primers and thermocycling parameters is provided in Supplementary Table S2. Bacterial:fungal (B:F) ratios were calculated as the quotient of bacterial to fungal gene copy numbers, providing an index of microbial community composition that is independent of enzyme activity measurements.

Analysis of peat enzymatic activities

FDA hydrolase activity was quantified by incubating 0.05 g of air-dried peat with fluorescein diacetate, and the hydrolysed fluorescein was measured at 490 nm following centrifugation (Biorbyt Ltd., FDA Assay Kit, orb1499582). UA activity was determined using the indophenol blue colorimetric method, where 0.05 g of air-dried peat was incubated with urea at 37 °C for 24 h, and the resulting ammonium concentration was measured at 630 nm (Biorbyt Ltd., Urease Assay Kit, orb545636). ACP activity was assessed by incubating 0.1 g of air-dried peat with p-nitrophenyl phosphate at 37 °C for 15 min, and the resulting p-nitrophenol was quantified at 510 nm (Biorbyt Ltd., Acid Phosphatase Assay Kit, orb219857). We used 37 °C following standardised commercial kit protocols to ensure inter-kit reproducibility and comparability with the extensive soil enzyme literature. While this exceeds field temperatures at Moor House (MAT ~ 6 °C; July maximum 12.3 °C), we prioritise relative enzyme allocation (UA:ACP ratios) rather than absolute in situ rates. The 37 °C temperature standardises activities across samples, eliminating temperature as a source of variation while amplifying signal detection from low-activity peat. Temperature sensitivity is generally proportional across enzyme classes within soil types (Koch et al. 2007), suggesting UA:ACP ratios should be preserved even if absolute activities differ from field conditions. For each enzyme assay, standard curves were generated using at least six concentrations of standard solutions, achieving R^2 values consistently between 0.98 and 1.00. We employed multiple controls to ensure measurement accuracy, including substrate blanks (buffer + substrate without peat) to correct for spontaneous substrate hydrolysis, sample blanks (peat + buffer without substrate) to correct for background absorbance from peat organic matter, and negative controls to confirm absence of contamination. Killed controls (autoclaved peat) were not included; the implications of this are discussed in Sect. "Methodological considerations and the robustness of enzymatic stoichiometric ratios".

To minimise potential artifacts and ensure comparability, all samples underwent identical processing, including air-drying at room temperature for 48 h, homogenisation, storage at 4 °C, and analysis within 7 days of drying. This standardised protocol ensures that any drying effects are consistent across all seasonal, elevational, and depth treatments, allowing valid comparisons of relative enzyme allocation patterns within our dataset (Dunn et al. 2014; Lopes et al. 2015). However, absolute UA:ACP values and derived thresholds should be considered method-specific to air-dried peat analysed at 37 °C and require validation using field-moist samples with killed controls before application to other systems.

Statistical analysis

Due to the non-normal distribution of the data, as confirmed by Shapiro–Wilk tests, non-parametric statistical methods were applied. The Mann–Whitney U test was applied for seasonal comparisons of peat physicochemical properties. The significance of differences across elevation and depth was tested using Kruskal–Wallis rank sum tests, while Spearman's rank correlation coefficients were used to assess correlations between variables.

Partial Least Squares Path Modelling (PLS-PM) was applied to assess the relationships among soil physicochemical properties, microbial abundance, enzymatic activities, and spatiotemporal factors of season and elevation. The PLS-PM model was structured hierarchically, with spatial and seasonal factors as exogenous variables (Level 1), peat physical properties, nutrient contents, and microbial abundance as mediating variables (Level 2), elemental and enzymatic stoichiometries as endogenous variables (Level 3). Path relationships were specified based on ecological hypotheses. Path coefficients were estimated using bootstrapping with 500 iterations, identifying significant relationships and quantifying the strength of effects. Coefficient of determination (R^2) was used to assess the variance explained in the dependent variables. Path coefficients (β values) represent the strength and direction of relationships between latent variables, and their significance was evaluated using bootstrapped p-values. Model performance was further evaluated through Goodness-of-Fit (GoF) index.

Variation Partitioning Analysis (VPA) and Hierarchical Partitioning (HP) were further employed to evaluate the shared variance and relative importance of specific variables from PLS-PM level 2 in regulating stoichiometric relationships. VPA was conducted to partition the total explained variance among nutrient contents, peat physicochemical properties, and microbial abundance. Redundancy analysis (RDA) with 4,999 permutations was used to test the significance of unique and shared fractions. The total variance was divided into unique, joint, and residual components, with the residual fraction representing unexplained variability. The relative explanatory power of each component was expressed as the proportion of total variance explained, providing a quantitative basis for identifying the dominant environmental and microbial drivers of stoichiometric variation. Prior to HP analysis, a Spearman correlation matrix was computed among all predictors to assess and filter the selected variables, thereby minimising potential collinearity issues. HP was then applied to quantify the independent contributions of individual predictors, including nutrient contents (NH_4^+, NO_3^-, PO_4^{3-}) and peat physicochemical properties (temperature, pH, EC, and water content), to the variation in N:P and UA:ACP ratios. Independent effects were estimated based on goodness-of-fit (R^2) values, and their statistical significance was assessed through 1,000 randomised permutations.

A power-law model was used to quantify the relationship between N:P ratios and UA:ACP ratios. To linearise the relationship, both variables were log-transformed and fitted using a simple linear regression model log (UA:ACP ratio) = $\alpha + \beta$log (N:P ratio). The intercept (α) and slope (β) were estimated, and then back-transformed to obtain the equation on the original scale as UA:ACP = $a\ x$ (N:P)^b, where $a = e^\alpha$ and $b = \beta$. Model fit was assessed using the coefficient of determination (R^2) and the p-value of the slope term. Uncertainty around the predicted curve was estimated by non-parametric bootstrapping (1,000 resamples) to generate 95% confidence intervals.

Maps were generated using ArcGIS Pro version 3.0.2. All analyses were carried out using RStudio version 4.4.1 with the *ggplot2* (Wickham 2016), *dplyr* (Wickham et al. 2023), *vegan* (Oksanen et al. 2022), *hier.part*, *lme4* (Bates et al. 2015), *ggforce* (Pedersen 2022), *MuMIn* (Bartoń

2023), *mgcv* (Wood 2000), *stats* (R core Team 2012) and *plspm* (Sanchez 2013) packages.

Results

Seasonal and spatial variation in elemental and enzymatic stoichiometries

Figure 2A demonstrates that elemental N:P ratios were significantly higher in summer than in winter across all depths ($n = 20$ per season at each depth; $p < 0.001$). At 0–20 cm, mean N:P values increased from 11.36 ± 2.75 in winter to 42.26 ± 7.40 in summer. At 20–40 cm, means increased from 13.35 ± 3.03 to 78.15 ± 9.55 in summer, and at 40–60 cm from 26.01 ± 4.48 to 102.40 ± 29.92. These patterns indicate a strong seasonal shift in N:P stoichiometry, with summer peat showing pronounced N enrichment, while winter peat remained consistently lower and clustered around or below the canonical N:P threshold of 16, consistent with conditions typically associated with relative N limitation at the ecosystem level.

In contrast, Fig. 2B shows that UA:ACP ratios were significantly higher in winter than in summer across all depths ($n = 20$ per season at each depth; $p < 0.001$). Winter values averaged 283.53 ± 14.21 at 0–20 cm, 191.54 ± 47.59 at 20–40 cm, and 38.52 ± 10.87 at 40–60 cm, while summer values were much lower, averaging 59.73 ± 10.94, 21.37 ± 4.58, and 12.74 ± 6.30, respectively. This inverse seasonal pattern, high N:P with low UA:ACP in summer, and low N:P with high UA:ACP in winter, suggests reciprocal shifts in plant nutrient status and microbial enzyme allocation strategies between seasons.

Stoichiometric and enzymatic ratios exhibited strong and contrasting depth-dependent patterns (Fig. 3). N:P ratios increased markedly with depth in both seasons, with values at 40–60 cm approximately doubling relative to surface layers. In winter, N:P increased from 13.23 ± 0.85 at 0–20 cm to 27.91 ± 1.03 at 40–60 cm (~ 2.1-fold increase), while in summer, it rose from 33.93 ± 2.71 to 90.06 ± 6.49 (~ 2.7-fold increase). In contrast, UA:ACP ratios showed the opposite trend, declining sharply with depth. In winter, UA:ACP decreased from 283.53 ± 14.21 at 0–20 cm to 38.52 ± 10.87 at 40–60 cm (~ 7.4-fold decrease), whereas in summer, it declined from 59.73 ± 10.94 to 12.74 ± 6.30 (~ 4.7-fold decrease). These depth-driven changes were statistically significant, with the deepest layer consistently differing from surface soils for both ratios.

Using a threshold of UA:ACP = 88 (derived from the power-law relationship in Sect. "Elemental-Enzymatic Coupling Across Environmental Gradients"), nearly all winter values from the top two layers exceeded this

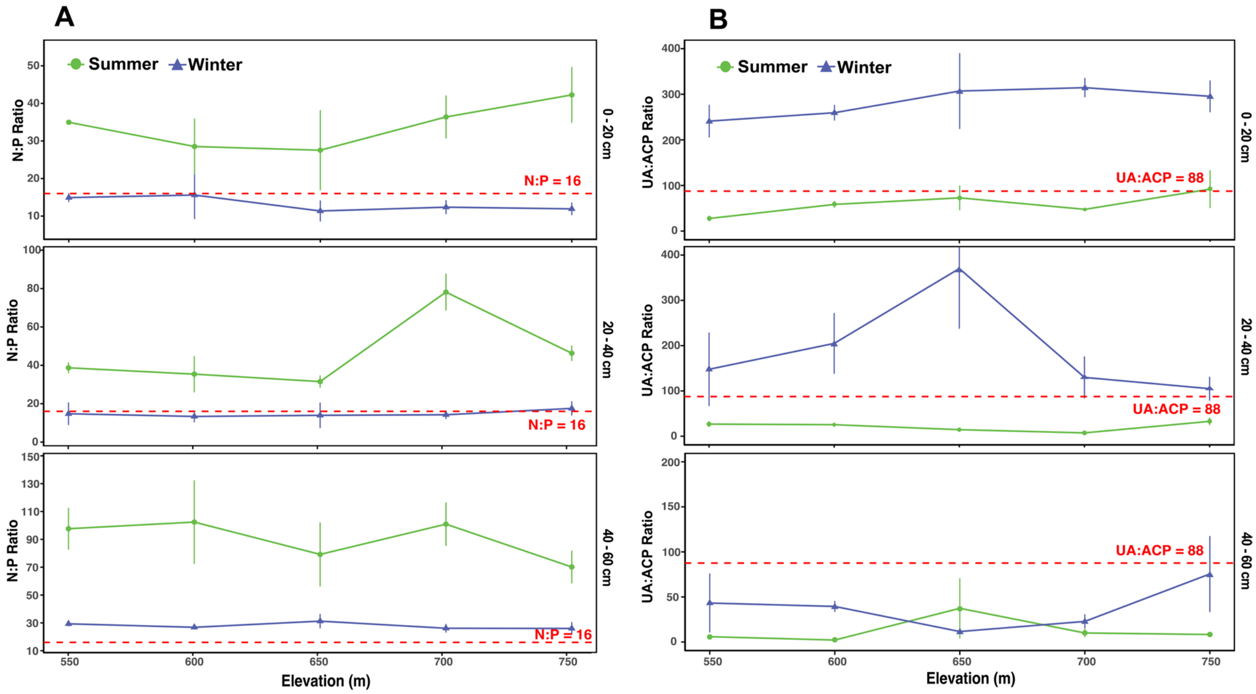

Fig. 2 Seasonal and depth variation in (**A**) N:P ratios and (**B**) UA:ACP ratios across elevation gradients. Panel A shows N:P ratios with the threshold value of 16 (red dashed line), representing the canonical plant-based N:P benchmark and used here as a reference for relative nutrient balance at the ecosystem level. Panel B shows UA:ACP ratios with the threshold value of 88 (red dashed line) indicating the empirically derived transition in microbial enzymatic allocation based on the power-law relationship in Fig. 7. Error bars represent standard error of the mean (± SE). Sample size $n = 20$ per season × depth (5 elevations × 4 replicates, individual cores)

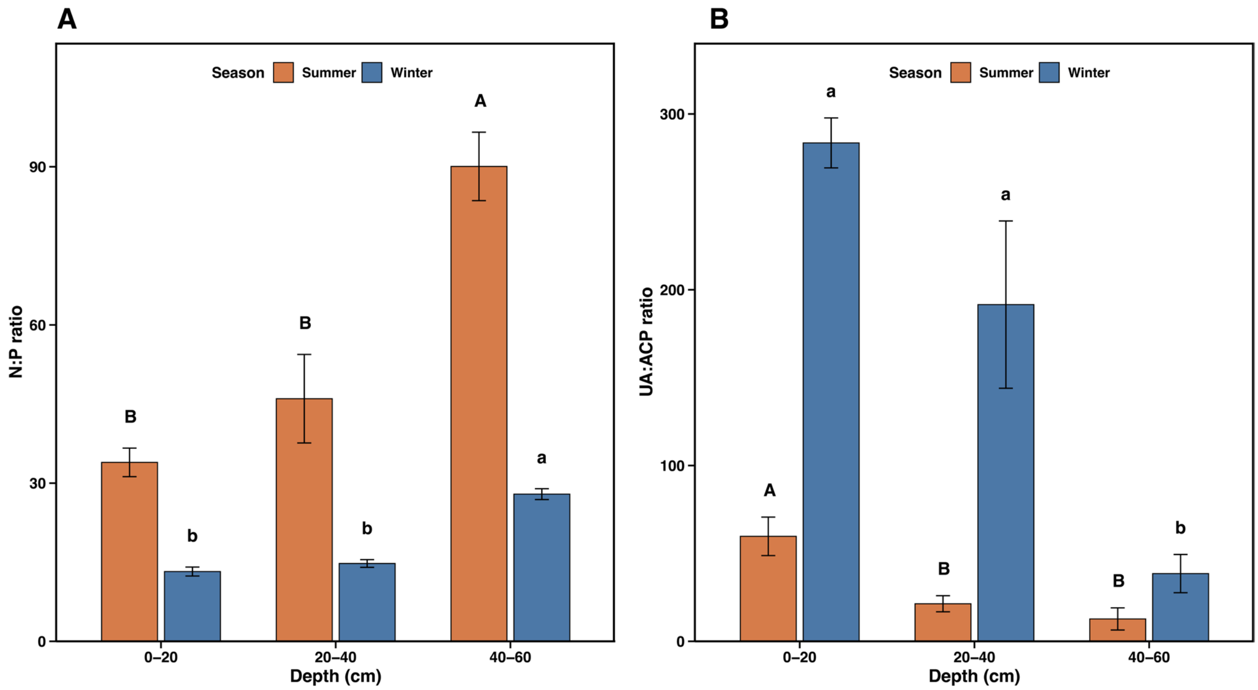

Fig. 3 Depth-dependent variation in peat stoichiometry. Mean (**A**) N:P ratios and (**B**) UA:ACP ratios across depth intervals (0–20, 20–40, 40–60 cm) for summer and winter. N:P increases with depth, while UA:ACP decreases down-profile across both seasons, showing consistent vertical gradients. Error bars represent ± SE. Uppercase letters (A, B) denote significant differences among depth intervals within summer, and lowercase letters (a, b) denote significant differences among depth intervals within winter ($p < 0.05$). Depths sharing the same letter are not significantly different

benchmark (100% at 0–20 cm and 65% at 20–40 cm), whereas exceedance was rare in summer (15% and 0%, respectively). In the 40–60 cm layer, only 10% of winter values and 5% of summer values exceeded the threshold, indicating that the seasonal contrast was strongest in the upper peat layers and diminished with depth.

Microbial community composition corroborated these stoichiometric patterns. B:F ratios were 4.3-fold higher in winter ($2.84 \times 10^3 \pm 7.77 \times 10^2$) than summer ($6.67 \times 10^2 \pm 3.44 \times 10^2$), with the strongest contrast in surface peat (18.9-fold; winter = $2.93 \times 10^3 \pm 8.14 \times 10^2$, summer = $1.55 \times 10^2 \pm 4.47 \times 10$). B:F ratios correlated negatively with N:P ratios (Spearman ρ = -0.407, $p < 0.05$) and UA:ACP ratios (Spearman ρ = -0.387, $p < 0.05$). In surface peat, this relationship was stronger, with B:F negatively correlated with N:P (Spearman $\rho = -0.709$, $p < 0.05$). These community shifts are consistent with bacterial competitive advantage under N limitation and fungal dominance under P limitation (Strickland and Rousk 2010). However, these relationships became non-significant when analysed within individual seasons, indicating that B:F ratios respond to broader environmental gradients rather than directly tracking nutrient limitation at finer scales. The observed shifts are therefore consistent with the stoichiometric patterns, while also likely influenced by additional factors such as temperature, redox conditions, and substrate quality.

Environmental drivers of stoichiometry variation

Given the pronounced seasonal and depth-related variation in stoichiometric ratios (Sect. "Seasonal and spatial variation in elemental and enzymatic stoichiometries"), we used PLS-PM to identify the hierarchical pathways through which environmental factors influence nutrient stoichiometry. The PLS-PM model in Fig. 4 achieved a moderate overall GOF of 0.48, providing a holistic view of how seasonal and spatial factors propagate through physicochemical, biological, and stoichiometric pathways. The model explained 77.2% of the variance in peat physical properties, 46.5% in nutrient content, 61.4% in microbial abundance, 38.7% in peat elemental stoichiometry, and 33.3% in enzymatic stoichiometry. Season emerged as the strongest driver, exerting positive effects on physical properties ($\beta = 0.84$, $p < 0.001$) and microbial abundance ($\beta = 0.76$, $p < 0.001$). Depth had strong negative effects on nutrient content ($\beta = -0.47$, $p < 0.001$) and microbial abundance ($\beta = -0.16$, $p < 0.05$), while elevation negatively influenced peat physical properties ($\beta = -0.27$, $p < 0.001$) and nutrient content ($\beta = -0.16$, $p < 0.05$). Within the enzymatic stoichiometry block,

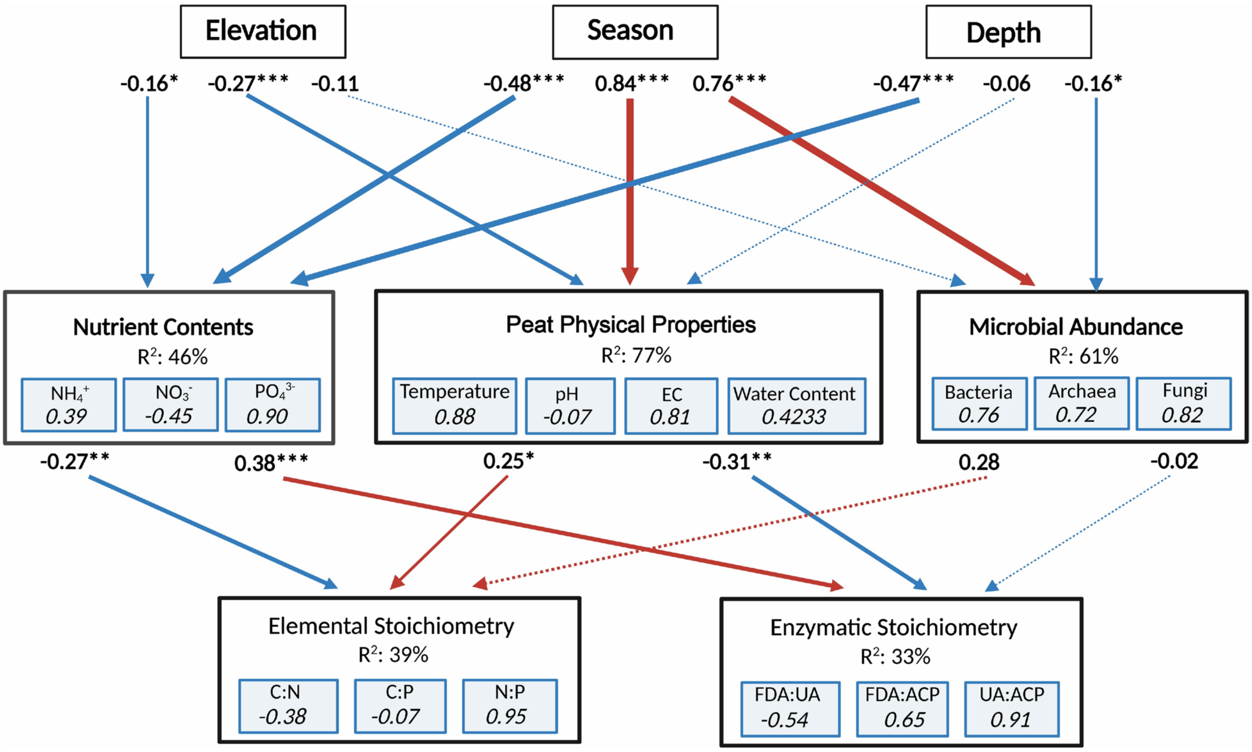

Fig. 4 PLS-PM linking environmental drivers to peat stoichiometry. Environmental factors (elevation, depth, season) influence intermediate latent constructs: Physicochemical Properties (temperature, EC, water content, pH), Nutrient Content (NH_4^+, NO_3^-, PO_4^{3-}), and Microbial Biomass (bacteria, archaea, fungi), which subsequently affect Peat Elemental Stoichiometry (C:N, C:P, N:P) and Enzymatic Stoichiometry (FDA:UA, FDA:ACP, UA:ACP). Path coefficients are shown as arrows: red lines represent positive relationships, blue lines represent negative relationships. Solid arrows indicate statistically significant paths ($p < 0.05$); dashed arrows denote non-significant relationships. Arrow thickness is proportional to effect size (β). R^2 values indicate variance explained in each endogenous variable. Values in italics within boxes show indicator loadings. Significance: *$p < 0.05$, **$p < 0.01$, ***$p < 0.001$

the UA:ACP ratio showed the highest loading (0.91), highlighting it as the most representative indicator of shifts in enzymatic allocation. This ratio approach was adopted deliberately. In water-saturated peat (averaging 86% moisture; Supplementary Table S3), enzyme ratios are expected to be more robust to assay artifacts than absolute activities, as systematic biases that affect both enzymes similarly cancel when expressed as ratios.

At the intermediate level, peat physical properties positively influenced peat elemental stoichiometry ($\beta = 0.25$, $p < 0.05$) but negatively influenced enzymatic stoichiometry ($\beta = -0.31$, $p < 0.01$). Conversely, nutrient content negatively affected elemental stoichiometry ($\beta = -0.27$, $p < 0.01$) but positively affected enzymatic stoichiometry ($\beta = 0.38$, $p < 0.001$). Microbial abundance had no significant direct effects on either stoichiometric component. Within the elemental stoichiometry block, N:P ratio showed the highest loading (0.95), indicating it was the strongest contributor to this latent construct. Similarly, within the enzymatic stoichiometry block, the UA:ACP ratio showed the highest loading (0.91), highlighting it as the most representative indicator of shifts in enzymatic allocation.

Given the dominant loadings of the N:P and UA:ACP ratios within their respective stoichiometric constructs, VPA was conducted to further explore how Level 2 components jointly influenced these representative ratios. For the N:P ratio (Fig. 5A), the three components collectively explained 35.2% of the total variance, leaving 64.8% as residuals. Among the unique fractions, peat physicochemical properties accounted for the largest share (8.1%, $p < 0.01$), followed by nutrient contents (7.6%, $p < 0.01$) and microbial abundance (0.4%, $p > 0.05$). Significant shared effects were observed between nutrients and physicochemical properties (1.3%, $p < 0.01$) and among all three components (9.0%, $p < 0.001$). For the UA:ACP ratio (Fig. 5B), the three components explained 31.1% of the total variance, with 68.9% remaining as residuals. Unique effects were dominated by nutrient contents (11.4%, $p < 0.01$), followed by peat physicochemical properties (3.9%, $p > 0.05$). Joint fractions between nutrients and physicochemical properties (7.5%, $p < 0.001$) and among

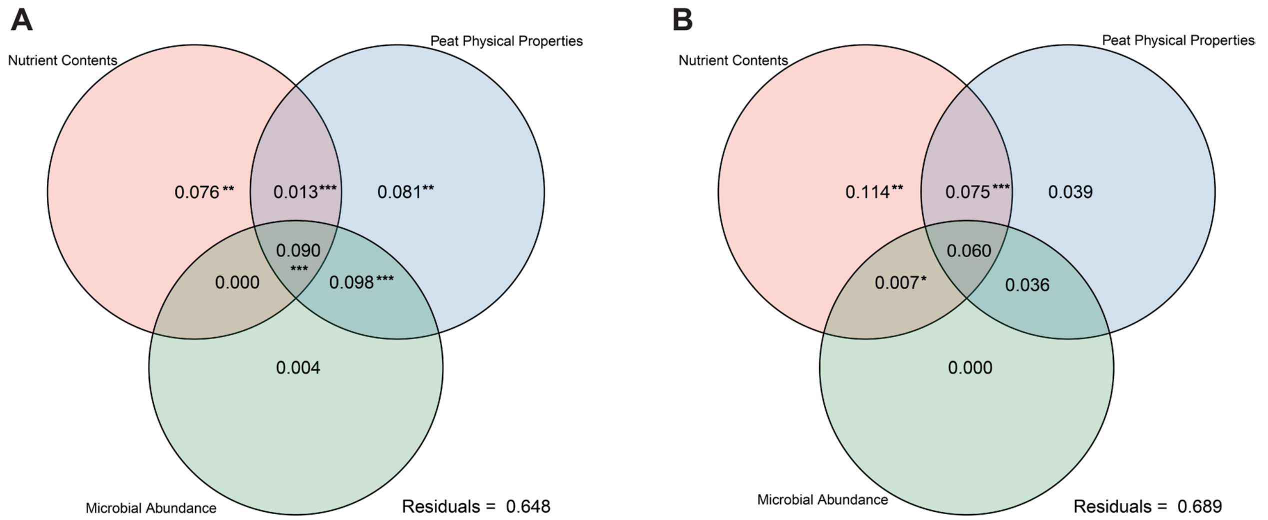

Fig. 5 Variation partitioning analysis showing unique and shared contributions of peat physical properties, nutrient contents, and microbial abundance to (**A**) N:P ratios and (**B**) UA:ACP ratios. Overlapping regions represent shared explanatory power; non-overlapping areas indicate unique contributions. Values shown are proportions of total variance. Residuals represent unexplained variance. Significance: *$p < 0.05$, **$p < 0.01$, ***$p < 0.001$

all three components (6.0%, $p < 0.01$) further emphasised the integrative control of nutrient and abiotic factors on enzymatic stoichiometric variation. Together, these results reinforce the PLS-PM findings, showing that nutrient availability and peat physicochemical conditions are the predominant drivers of stoichiometric adjustments, while microbial abundance exerts comparatively weaker effects.

Prior to HP analysis, a Spearman correlation matrix was examined to evaluate potential collinearity among predictors (Supplementary Fig. 3). Strong positive correlations were observed between temperature, bacterial abundance, and fungal abundance ($|\rho| > 0.6$), suggesting potential multicollinearity among microbial variables. To avoid spurious variance attribution, microbial abundance was therefore excluded from the HP models, ensuring reliable estimation of independent environmental effects. HP analysis was then applied to quantify the individual contributions of nutrient and physicochemical predictors to stoichiometric variation. For the N:P ratio (Fig. 6A), temperature, PO_4^{3-}, and EC exhibited the largest independent effects, explaining approximately 45%,

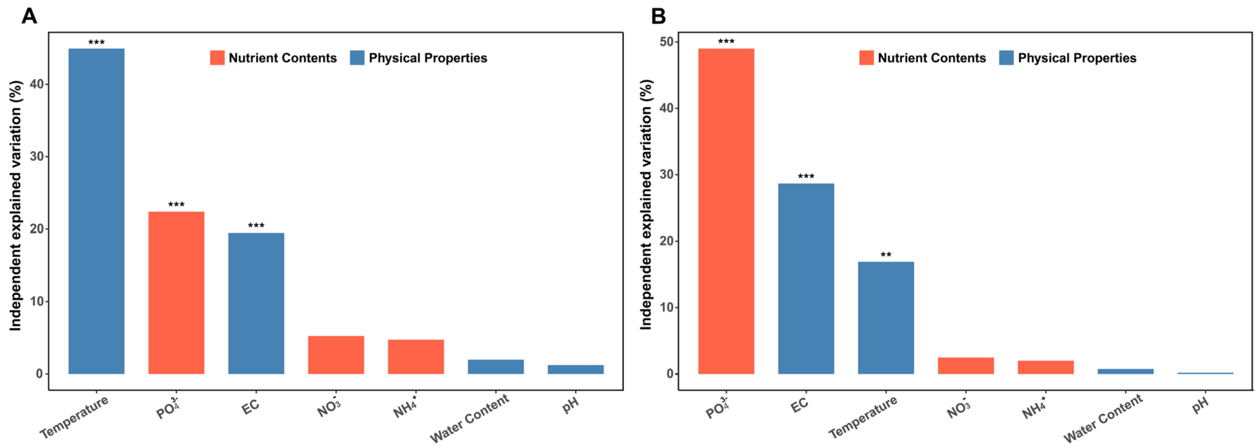

Fig. 6 Hierarchical partitioning analysis showing independent contributions of environmental variables to (**A**) N:P ratios and (**B**) UA:ACP ratios. Bars represent the percentage of variance explained independently by each predictor after accounting for effects of other variables. Nutrient contents include NH_4^+, NO_3^-, and PO_4^{3-}; physical properties include temperature, pH, EC, and water content. Significance determined by 1,000 randomised permutations: *$p < 0.05$, **$p < 0.01$, ***$p < 0.001$

22%, and 19% of the total variance, respectively, whereas NH_4^+, NO_3^-, pH, and water content contributed minimally (< 10%) and were not significant (all $p > 0.05$). For the UA:ACP ratio (Fig. 6B), PO_4^{3-} accounted for the strongest independent effect (49%), followed by EC (29%) and temperature (17%), while other variables showed negligible contributions.

Elemental-enzymatic coupling across environmental gradients

To establish the mechanistic link between plant nutrient status (N:P ratios) and microbial enzyme allocation (UA:ACP ratios) that underlies the seasonal patterns in Sect. "Seasonal and spatial variation in elemental and enzymatic stoichiometries", we examined their relationship across all samples and environmental conditions. Figure 7 illustrates a strong inverse power-law relationship between N:P and UA:ACP ratios ($n = 120$; $R^2 = 0.604$; $p < 0.001$), described by the equation:

$$UA : ACP \text{ Ratio} = 6.63 \times 10^3 \times N : P \text{ Ratio}^{-1.56}$$

UA:ACP ratios were highest at low N:P values and declined steeply with increasing N:P, approaching minimal levels at the upper N:P range. The data points were widely dispersed at low N:P ratios but became tightly clustered at high N:P, reflecting decreasing variability in UA:ACP with increasing N:P ratios. Winter samples were predominantly distributed at the low N:P and high UA:ACP end of the curve, whereas summer samples were mainly concentrated at the high N:P and low UA:ACP end.

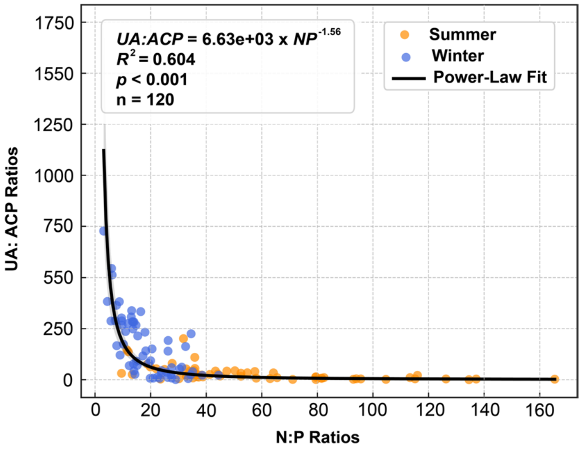

Fig. 7 The relationship between blanket bog ecosystems' elemental and enzymatic stoichiometries. Orange and blue points represent samples from summer and winter, respectively (n = 120). The curve represents the fitted power-law model, which explained 60.4% of the variation. Shaded bands represent the 95% confidence intervals around the fitted curve

Discussion

Environmental drivers structuring peatland biogeochemical frameworks

The observed variation in peat elemental and enzymatic stoichiometry reflects the superposition of processes operating over distinct temporal and spatial scales. On the one hand, seasonal dynamics drive rapid and reversible changes in nutrient availability through hydrothermal forcing, redox fluctuations, plant uptake, and microbial activity. On the other hand, depth-related gradients reflect long-term peat development, including progressive humification, selective nutrient loss, and the accumulation of recalcitrant organic matter. Distinguishing between these two axes of variation is essential for interpreting the magnitude and ecological significance of the stoichiometric patterns observed in this study.

Seasonal hydro-thermal forcing establishes the primary control on short-term biogeochemical dynamics in surface peat. In blanket bogs, warmer and relatively drier periods enhance oxygen availability and concentrate solutes in the upper peat layers, whereas cooler, water-saturated conditions maintain anoxia and dilute porewater chemistry. Temperature and EC jointly drive the cyclic restructuring of elemental and enzymatic stoichiometry in peatlands. They share some variance ($|\rho| = 0.44$, $p < 0.001$; Supplementary Fig. 3), reflecting their common response to seasonal hydro-thermal forcing, with temperature governing biological activity and EC representing the associated chemical reorganisation of porewater (Ponziani et al. 2012; Weedon et al. 2014; Machmuller et al. 2016). Specifically, elevated temperature accelerates litter decomposition and N mineralisation while stimulating oxidative enzymes that relax the phenolic/enzymic latch (Freeman et al. 2004). Enhanced microbial metabolism increases nutrient turnover and oxygen demand, while concurrent plant growth intensifies nutrient uptake, especially of PO_4^{3-}, tightening P supply relative to N (Wang and Moore 2014). In parallel, elevated EC likely arises from the accumulation of dissolved cations such as Ca^{2+}, Mg^{2+}, Fe^{2+}, and Al^{3+} derived from mineral weathering, atmospheric deposition, and ion exchange within peat (Urban et al. 1995; Comas and Slater 2004). The resulting increase in ionic strength enhances phosphate sorption through cation bridging and the formation of cation–P complexes (Xiong and Mahmood 2010; Tang et al. 2025), thereby reducing P bioavailability and shifting enzymatic allocation through ionic stress or substrate binding effects. Moreover, EC may reflect diffusion limitations on microbial activity in water-saturated peat environments (Fülöp et al. 2025), further linking ionic conditions to enzyme production patterns. Under oxic and warmer, conditions these processes intensify, whereas cooler, water-saturated, and reducing conditions suppress microbial activity, lower EC, and favour redox-driven processes, which releases previously bound phosphate. This interplay explains why EC accounted for a greater proportion of variation in UA:ACP ratios (29%) than temperature (17%), reflecting its closer association with PO_4^{3-} availability, which explained 49% of the variance and represents the dominant control of microbial enzymatic stoichiometry.

Oxygen limitation further constrains peatland biogeochemistry, particularly under water-saturated conditions. The high moisture content of blanket bogs (averaging 86% in our samples; Supplementary Table S3) creates steep vertical oxygen gradients that limit aerobic enzyme activity and constrain microbial metabolism (Freeman et al. 2001). Seasonal variation in water-table position modulates oxygen availability, with summer conditions enabling aerobic decomposition in surface peat and winter conditions maintaining predominantly anaerobic conditions. These redox dynamics interact with nutrient limitation by regulating access to phenolic-bound substrates and controlling the expression of oxidative enzymes associated with the "enzymic latch" (Freeman et al. 2004; Urbanová and Hájek 2021).

In contrast to these rapid seasonal processes, depth-related stoichiometric gradients reflect long-term diagenetic transformations associated with peat accumulation. With increasing depth, peat profiles become cooler and more anoxic (Fenner and Freeman 2011) and are enriched in humified, recalcitrant substrates (Moore and Dalva 2001; Tfaily et al. 2014; Drollinger et al. 2020). Oxygen diffusion limitations constrain enzyme–substrate interactions (Freeman et al. 2001; Wallenstein and Burns 2011), leading to declines in potential enzymatic activity and reduced capacity for rapid microbial reallocation (Pinsonneault et al. 2016; Steinweg et al. 2018; Urbanová and Hájek et al. 2021). Our results indicate that seasonal oscillations in elemental and enzymatic stoichiometry were pronounced in surface peat but diminished substantially below 40 cm, where variability was much weaker (Steinweg et al. 2018). Depth-related changes were particularly evident for P-related stoichiometry, N:P increasing threefold between 0–20 cm and 40–60 cm, consistent with progressive P depletion and humification during peat development. In deeper peat layers, bulk stoichiometry increasingly reflects the long-term imprint of accumulation and decomposition processes, and may therefore be partially decoupled from contemporary plant nutrient demand. Our sampling was limited to the upper 60 cm (approximately 20–33% of the total peat profile), missing the deeper peat horizons (60–300 cm) where the most recalcitrant organic matter resides and where microbial activity is substantially lower (Steinweg et al. 2018).

Elevation modifies these patterns by influencing both climate and atmospheric deposition. Across the studied elevational gradient (~ 200 m), the corresponding temperature decrease (~ 1.3 °C; Burt and Holden 2010) and variation in precipitation inputs influence peat physical properties and nutrient distributions. Higher-elevation sites experience enhanced cloud water deposition and greater hydrological connectivity, facilitating nutrient transport, particularly for dissolved N species (Cape et al. 2015; Mozafari et al. 2023). However, statistical analyses indicate that elevational effects were generally weak and variable. The clearest pattern was observed for NH_4^+ concentrations, which declined strongly with elevation in winter ($R^2 = 0.94$, $p < 0.01$ for 0–20 cm; Supplementary Table 3), whereas most other variables showed non-significant or inconsistent trends across elevation gradients and depth layers (Supplementary Tables 4–5).

These findings indicate that peatland stoichiometry is structured along two orthogonal axes: a dynamic seasonal axis governing short-term nutrient cycling and microbial enzyme allocation in surface peat, and a depth-dependent axis reflecting long-term peat development and constraining the baseline stoichiometric composition of the system.

Methodological considerations and the robustness of enzymatic stoichiometric ratios

Enzyme assays in peatlands present unique methodological challenges compared to mineral soils because of the high water content and distinct physicochemical properties of peat. Our samples averaged 85.7 ± 6.8% moisture (range: 70.9–91.0%; Supplementary Table S3), meaning fresh peat consists primarily of pore water with organic matter forming a suspended or semi-solid matrix. While air-drying reduces absolute activities, we employed a standardised protocol to ensure that relative differences across seasons and depths were preserved, allowing for valid comparisons of enzyme allocation patterns. A detailed evaluation of these methodological complications and our justification for using air-dried samples is provided in Supplementary Text S1.

Despite these constraints, multiple lines of evidence indicate that our enzyme metrics reflect ecological signals rather than being dominated by methodological artefacts. Recent reviews have questioned the validity of using enzyme activity ratios to infer nutrient limitation (Rosinger et al. 2019; Mori 2020; Mori et al. 2023), particularly in C:N:P frameworks where β-glucosidase is used as a proxy for C acquisition, even though it also contributes to N acquisition via chitin degradation (Mori et al. 2021). Our framework avoids these confounding effects by focusing exclusively on N:P limitation within a C-rich system (peat averaging 44%, Supplementary Table S5), where microbial enzyme allocation responds primarily to relative N versus P scarcity rather than absolute C availability. The biological validity of this approach is confirmed by hierarchical partitioning, which showed that porewater chemistry variables (PO_4^{3-}, EC, temperature) explained the dominant share of variation in both N:P and UA:ACP ratios (Fig. 6). For UA:ACP specifically, PO_4^{3-} accounted for 49% of variance, followed by EC (29%) and temperature (17%), indicating that enzyme allocation patterns track biogeochemical conditions. Furthermore, the tight power-law relationship between N:P and UA:ACP ($R^2 = 0.60$, $p < 0.001$; Fig. 7) and the clear seasonal separation in surface peat ((winter mean = 237 vs summer mean = 59; Fig. 2) demonstrate that enzyme stoichiometry tracks nutrient limitation status across contrasting peatland treatments, seasons, and depths. These correlations would be unlikely if enzyme ratios were primarily determined by assay artefacts rather than biological regulation. Nonetheless, absolute UA:ACP values and the derived threshold (UA:ACP = 88, 95% CI: 64–118) should be treated as method-specific until validated under field-moist conditions and alternative assay controls (e.g. killed controls, in situ assays) are applied.

Importantly, these enzyme patterns are further supported by microbial community composition shifts. B:F ratios were 4.3-fold higher in winter than summer (18.9-fold in surface peat), consistent with the observed seasonal stoichiometric gradients. This coherence across pore-water chemistry (PO_4^{3-} explains 49% of UA:ACP variance), elemental stoichiometry (N:P–UA:ACP, $R^2 = 0.60$), and microbial community composition demonstrates that enzyme allocation patterns reflect ecosystem nutrient status. Integrating microbial community ratios with enzyme stoichiometry strengthens the elemental–enzymatic coupling framework in two key ways. First, it shows that the framework captures processes operating across biological scales, from molecular (enzyme allocation) to community (bacterial vs fungal dominance). Second, it provides a validation pathway that is independent of the specific methodological constraints affecting enzyme assays (air-drying, incubation temperature). Although B:F ratios measured by qPCR carry their own biases (e.g. differential DNA extraction efficiency for bacteria and fungi; inability to distinguish dead from live cells), their close correspondence with enzyme allocation patterns suggests that both metrics respond to the same underlying nutrient limitation gradient. This multi-scale convergence is consistent with expectations if our framework accurately diagnoses ecosystem nutrient status.

Elemental-enzymatic coupling as an inverse power-law mechanism

The N:P thresholds of < 14 and > 16 used in this study originate from plant stoichiometric frameworks, where they have been widely applied to diagnose N versus P limitation in vegetation (Güsewell 2004; Ptacnik et al. 2010; Wang and Moore 2014). In the present study, these thresholds are not interpreted as direct indicators of plant physiological limitation, but rather as heuristic reference points for ecosystem-level nutrient balance. Under this framework, the plant-derived thresholds serve as anchor points within a broader stoichiometric continuum, allowing inference of relative N versus P constraint at the ecosystem scale, where nutrient availability emerges from the combined effects of plant inputs, microbial processing, and long-term peat accumulation. While this approach necessarily simplifies the complexity of ecosystem nutrient dynamics, the close alignment between elemental and enzymatic indicators in this study suggests that these thresholds retain functional relevance beyond plant tissues, particularly when interpreted in conjunction with microbial activity.

Before interpreting the power-law relationship, we acknowledge that UA represents one of multiple microbial pathways for N acquisition in peatlands. In natural ecosystems, organic N mobilization depends primarily on polymer-degrading enzymes including N-acetyl-β-glucosaminidase (NAG), leucine aminopeptidase (LAP), and other peptidases that break down proteins and chitin (Parvin et al. 2018; Zhai et al. 2025). UA, which hydrolyses urea to ammonium, is most relevant in agricultural systems with synthetic fertiliser inputs, though it remains active in natural systems where urea derives from atmospheric deposition and microbial turnover (Motasim et al. 2024). Consequently, our UA:ACP thresholds should be interpreted as method-specific proxies for UA-based N acquisition rather than comprehensive microbial N limitation indicators. They likely underestimate total N-acquiring enzyme investment and represent a conservative lower bound for microbial N limitation. However, the strong coupling between bulk peat N:P ratios and microbial UA:ACP enzymatic allocation provides an independent, process-based indicator of nutrient demand. The robust correlation observed across seasons, depths and elevations confirms its utility as a reliable tracer of ecosystem nutrient status.

Our study demonstrates that elemental and enzymatic stoichiometries are coupled through an inverse power-law relationship, which carries two mechanistic implications. First, the negative exponent indicates that as the peat-plant system shifts toward higher N:P ratios, reflecting stronger relative P scarcity, microbes reduce the UA:ACP ratio by investing proportionally more in phosphatase relative to urease. Conversely, at low N:P, UA activity dominates while ACP is suppressed, resulting in a higher UA:ACP ratio. This pattern is consistent with optimal foraging theory, in which microorganisms adjust enzyme production to mitigate resource imbalances (Margalef et al. 2017; Mooshammer et al. 2014). Given the intrinsically high C content of peat, microbial enzyme allocation is therefore governed by the relative availability of N and P, with phosphatase production favoured under P limitation and UA favoured under N limitation (Sinsabaugh and Moorhead 1994). Second, the magnitude of the exponent (≈ -1.56) indicates strong sensitivity at low N:P and diminishing responsiveness at high N:P. Under N limitation, small reductions in N:P elicit large increases in the UA:ACP ratio, whereas responses saturate under pervasive P limitation. The dispersion pattern reinforces this mechanism where variability in UA:ACP is high under N scarcity, reflecting a broad portfolio of microbial strategies for N acquisition. Part of this variability may also reflect the influence of legacy P pools at depth, where accumulated and partially recalcitrant P can decouple bulk N:P ratios from immediately bioavailable P. This may introduce scatter in the N:P–UA:ACP relationship by weakening the linkage between bulk stoichiometry and microbial enzyme allocation, particularly in deeper peat layers. By contrast, variability converges under P limitation, when microbial strategies are constrained to enhanced phosphatase production, underscoring the specificity of ACP as a marker of P acquisition (Jian et al. 2016). Consistent with these findings, global analyses show that N enrichment can stimulate P-mediated P mobilisation without altering total or available P pools, indicating that P availability is buffered by enzymatic processes rather than directly reflected in bulk stoichiometry (Chen et al. 2020). Using established boundaries of $N:P < 14$ and $N:P > 16$, we derived specific microbial benchmarks where ratios of $UA:ACP = 108$ indicate N limitation and $UA:ACP = 88$ indicate P limitation. These thresholds provide a proof-of-concept framework linking elemental and enzymatic stoichiometry in peatlands. Although they carry statistical uncertainty, with 95% confidence intervals on the exponent (– 1.39 to – 1.73) propagate to the thresholds. At $N:P = 16$, the UA:ACP threshold's 95% confidence interval spans 64 to 118. Values between 70 and 110 should therefore be considered "near-threshold" rather than definitively N- or P-limited, though the clear seasonal separation in our data (winter mean = 237 vs. summer mean = 59 in surface peat) falls well outside this uncertainty range. Future work incorporating additional N-acquiring enzymes (NAG, LAP) would refine threshold quantification while preserving the underlying elemental-enzymatic coupling mechanism.

Ecological responses to seasonal and spatial nutrient dynamics

In blanket bog ecosystems, carbon limitation is unlikely in peat systems, where total organic C averages 44% (Supplementary Table S5), but energy limitation may occur when oxygen scarcity restricts aerobic respiration, forcing microbes to rely on less efficient anaerobic pathways. Therefore, shifts in the balance between N and P availability regulate plant community composition, microbial activity, and the efficiency of C storage.

Our study revealed that seasonality organises blanket-bog nutrient limitation along a consistent axis from winter N limitation to summer P limitation. The magnitude of these seasonal shifts is particularly pronounced in surface peat, where N:P ratios increased substantially between winter and summer, reflecting a transition toward stronger P constraint during the growing season. This pattern is consistent with the observed changes in microbial enzyme allocation, where increases in UA:ACP ratios indicate reduced relative investment in P-acquiring enzymes under conditions of elevated PO_4^{3-} availability, and a reallocation toward N processing. At the plant level, nutrient limitation governs both community composition and C storage efficiency. Under N limitation, *Sphagnum* mosses dominate because of their efficiency under low-N conditions, while vascular plants remain suppressed (Limpens et al. 2003, 2004). Although productivity is modest, *Sphagnum* provides a continuous input of recalcitrant litter that contributes substantially to peat accumulation and supports organic matter build-up (Temmink et al. 2023; Zhao et al. 2023). By contrast, when P becomes limiting, N enrichment promotes vascular plant expansion and reduces *Sphagnum* competitiveness (Chiwa et al. 2018). This shift alters litter quality toward more labile vascular plant material, enhancing decomposability and reducing the efficiency of long-term carbon storage (Moore et al. 2007; Zeh et al. 2020).

Microbial processes further mediate these ecosystem responses by regulating nutrient availability and organic matter turnover. In ombrotrophic bogs, where carbon content is particularly high, microbial activity plays a central role in controlling decomposition and nutrient cycling (Barta et al. 2025). Under N limitation, microbial metabolism is constrained, decomposition rates remain low, and C preservation is relatively stable (Luo et al. 2021). The restricted capacity for organic matter breakdown allows much of the C fixed by plants to remain stored in peat, contributing to high C content and sustained peat accumulation (Jayasekara et al. 2025). In contrast, a shift toward P limitation generally reflects the alleviation of N limitation under elevated N supply (Bragazza et al. 2010; Gao et al. 2022). Under these conditions, microbial activity intensifies, accelerating organic matter mineralisation and increasing C turnover (Song et al. 2017; Wieder et al. 2020).

P dynamics in these ombrotrophic systems reflect both contemporary atmospheric inputs (0.62–1.75 kg P ha^{-1} yr^{-1} at comparable UK sites; Worrall et al. 2016) and recycling of legacy P accumulated during peat development. While atmospheric deposition represents the dominant pathway for new P entering the system under current conditions, the underlying glacial till at Moor House likely contributed P through weathering during initial peat formation and may continue to do so at low rates in deeper layers. The measured total P concentrations (0.014–0.157%; Supplementary Table S5) represent this accumulated P pool, most of which now cycles internally through plant uptake, microbial processing, and decomposition rather than being supplied annually from the atmosphere. Seasonal shifts in bioavailable P may therefore reflect redox-mediated transformations rather than variable atmospheric inputs. During anoxic winter conditions, P is released from microbial biomass turnover and desorption from phenolic compounds in partially decomposed organic matter (Qin et al. 2024). Small quantities of Fe/Al, derived from both historical mineral weathering and ongoing atmospheric deposition, form organo-metallic complexes with humic substances that can also release P under reducing conditions (Yang et al. 2022; Curtinrich et al. 2022). Conversely, typically drier and oxic summer conditions promote P immobilisation through microbial uptake, complexation with phenolic groups, and sorption to organo-metallic sites (Zak et al. 2004). This distinction between P sources (historical accumulation from weathering and deposition) and P cycling (contemporary redox-mediated transformations) is important for interpreting seasonal N:P ratio shifts, as it indicates that nutrient limitation patterns are driven by bioavailability rather than absolute P scarcity.

Nutrient interactions further reinforce these dynamics through feedbacks involving biological N fixation. Higher PO_4^{3-} concentrations in our study coincided with increases in both N:P and UA:ACP ratios, a pattern consistent with P stimulation of diazotrophic activity. In *Sphagnum*-dominated systems, experimental additions of inorganic P substantially increase N_2 fixation rates (Van Den Elzen et al. 2017). Field observations further show that nutrient status, including P supply, regulates spatial and seasonal variability in biological N_2 fixation (Zivkovic et al. 2022). These findings support our interpretation that enrichment with PO_4^{3-} alleviates P limitation of diazotrophs, enabling greater N_2 fixation and thereby increasing ecosystem N relative to P.

While these responses are most strongly expressed in surface peat layers, spatial constraints, particularly with depth, limit the extent to which seasonal changes propagate through the peat profile. Deeper peat layers, shaped by long-term accumulation and decomposition processes, have greater stoichiometric stability and reduced microbial responsiveness, effectively buffering deeper C stores from rapid biogeochemical reorganisation. Consequently, seasonal shifts in nutrient limitation primarily influence the biologically active surface layer, while deeper peat maintains the longer-term structural and stoichiometric framework of the system. These results demonstrate that blanket-bog ecosystem functioning is governed by the interaction between dynamic seasonal forcing and spatial constraints imposed by peat development. Seasonal changes regulate the expression of nutrient limitation and associated biological processes in surface peat, while depth-dependent structure constrains their propagation. This coupling between temporal variability and spatial structure ultimately shapes nutrient cycling, microbial activity, and the long-term balance between carbon accumulation and decomposition in peatland ecosystems.

Applications and implications of the nutrient limitation threshold in bogs

The elemental-enzymatic threshold and framework developed in this study has important practical applications for peatland science and management. First, the application of the derived UA:ACP thresholds allows for a rapid classification of microbial nutrient states even when physicochemical data are unavailable. By identifying whether a system is under N pressure (exceeding the 108 benchmark) or P pressure (falling below the 88 benchmark), the functional status of the peat microbiome can be assessed more efficiently. Second, it provides a monitoring tool, as the frequency and persistence of threshold crossings can guide the design of seasonally informed management, such as reducing external N inputs in winter or limiting P immobilisation in summer. Third, it offers a parsimonious rule for models, improving predictions of plant–microbe interaction by linking enzyme allocation directly to elemental stoichiometry.

Nutrient limitation in these systems emerges from the interaction between dynamic seasonal forcing and spatial constraints imposed by peat development. Seasonal variability represents the dominant driver of short-term changes in nutrient availability and microbial function, particularly in the biologically active surface layer. In contrast, depth reflects long-term peat accumulation and diagenetic processes that establish the baseline stoichiometric framework within which these seasonal dynamics operate. As a result, while seasonal forcing controls the timing and expression of N versus P limitation, depth constrains its magnitude and propagation through the peat profile. Under projected warming and drying, seasonal effects are likely to intensify, prolonging periods of P limitation in surface peat and increasing the frequency of threshold crossings, with important consequences for ecosystem stability and long-term C sequestration.

This snapshot seasonal comparison (July 2023 and February 2024) provides proof-of-concept but cannot distinguish typical seasonal patterns from year-specific climate anomalies or characterise intra-seasonal transitions. The strong statistical relationships ($R^2 = 0.60$; clear seasonal differentiation in Fig. 2) suggest our patterns capture fundamental biogeochemical processes rather than stochastic variation, but multi-year validation is essential before applying this framework to predict responses to interannual climate variability. Future research should prioritise monthly sampling across multiple years, replication across multiple blanket bog sites spanning climatic gradients, and experimental manipulation to test causal mechanisms and validate that threshold crossings correspond to measurable ecosystem state changes. Furthermore, because our model was developed for ombrotrophic, rain-fed blanket bogs with inherently limited nutrient inputs, validation across other peatland types is also needed. Finally, we recommend including a wider range of N-acquiring enzymes in future assessments to refine the evaluation of nutrient limitation and strengthen its relationship with N:P ratios. While the absolute threshold values are method-specific and require validation across peatland types, the inverse power-law coupling between N:P and UA:ACP ratios represents a robust framework for integrating plant and microbial perspectives on nutrient limitation.

Abbreviations

ACP	Acid phosphatase
ANOVA	Analysis of variance
B:F	Bacterial-to-fungal ratio
CI	Confidence interval
C	Carbon
EC	Electrical conductivity
FDA	Fluorescein diacetate
GOF	Goodness-of-fit
N	Nitrogen
NH_4^+	Ammonium
NO_3^-	Nitrate
N:P	Nitrogen-to-phosphorus
P	Phosphorus
PLS-PM	Partial least squares path modelling
PO_4^{3-}	Phosphate
qPCR	Quantitative real-time polymerase chain reaction
UA	Urease
UA:ACP	Urease to acid phosphatase
VPA	Variation partitioning analysis

Supplementary Information

The online version contains supplementary material available at https://doi.org/10.1186/s13717-026-00700-w.

Additional file 1.

Acknowledgements

This study was financially supported by the UKRI Natural Environment Research Council (NERC) through the Central England NERC Training Alliance (CENTA2) Grant NE/S007350/1. Work by NM and DM at the Moor House (Environmental Change Network) site is supported by NERC, through the UKCEH National Capability for UK Challenges Programme NE/Y006208/1. We thank Natural England for access to the Moor House and for their support of long-term ecological research at the site. We thank Alex Thorpe and Simon Oakley for support with field sampling. Open access funding provided by University of Warwick.

Declaration of AI-assisted technologies in the manuscript preparation process

During the preparation of this work the authors used Microsoft Co-Pilot to improve language and readability. After using this tool, the authors reviewed and edited the content as needed and take full responsibility for the content of the published article.

Author contributions

SG: conceptualisation and design, investigation, methodology, formal analysis, visualisation, writing original draft; DT: methodology, writing, review and editing; DW: methodology, writing, review and editing; DM: methodology, writing, review and editing; NM: conceptualisation and design, supervision, writing, review and editing; GB: conceptualisation and design, supervision, writing, review and editing; RM: conceptualisation and design, investigation, supervision, writing, review and editing. All authors read and approved this manuscript.

Funding

UKRI Natural Environment Research Council, Central England NERC Training Alliance (CENTA2) Grant NE/S007350/1,UKCEH National Capability for UK Challenges Programme NE/Y006208/1,UKCEH National Capability for UK Challenges Programme NE/Y006208/1

Availability of data and materials

All data generated or analysed during this study are included in this published article and its Supplementary Tables S3–S6.

Declarations

Consent for publication

Not applicable.

Competing interests

The authors declare no competing interests.

Author details

[1]School of Life Sciences, University of Warwick, Coventry CV4 7AL, UK. [2]Centre for Ecology and Hydrology, Lancaster Environment Centre, Lancaster LA1 4AP, UK.

Received: 27 January 2026 Accepted: 19 April 2026

References

Adam G, Duncan H (2001) Development of a sensitive and rapid method for the measurement of total microbial activity using fluorescein diacetate (FDA) in a range of soils. Soil Biol Biochem 33(7–8):943–951. https://doi.org/10.1016/S0038-0717(00)00244-3

Armstrong A, Waldron S, Ostle NJ, Richardson H, Whitaker J (2015) Biotic and abiotic factors interact to regulate northern peatland carbon cycling. Ecosystems 18:1395–1409. https://doi.org/10.1007/s10021-015-9907-4

Arsenault J, Talbot J, Moore TR (2018) Environmental controls on C, N and P biogeochemistry in peatland pools. Sci Total Environ 631–632:714–722. https://doi.org/10.1016/j.scitotenv.2018.03.064

Avery BW (1990) Soils of the British Isles. CAB International, Wallingford, UK

Barta J, Santruckova H, Novak M, Cejkova B, Jackova I, Buzek F, Stepanova M, Curik J, Veselovsky F, Prechova E (2025) Microbial community dynamics in two Central European peatlands affected by different nitrogen depositions. FEMS Microbiol Ecol 101(7):fiaf056. https://doi.org/10.1093/femsec/fiaf056

Bartoń K (2023) MuMIn: multi-model inference. R package version 1.47.1. https://CRAN.R-project.org/package=MuMIn

Bates D, Mächler M, Bolker B, Walker S (2015) Fitting linear mixed-effects models using lme4. J Stat Soft 67(1):1–48. https://doi.org/10.18637/jss.v067.i01

Belyea LR, Malmer N (2004) Carbon sequestration in peatland: patterns and mechanisms of response to climate change. Glob Chang Biol 10:1043–1052. https://doi.org/10.1111/j.1529-8817.2003.00783.x

Bragazza L, Tahvanainen T, Kutnar L, Rydin H, Limpens J, Hájek M, Grosvernier P, Hájek T, Hajkova P, Hansen I, Iacumin P, Gerdol R (2004) Nutritional constraints in ombrotrophic *Sphagnum* plants under increasing atmospheric nitrogen deposition in Europe. New Phytol 163:609–616. https://doi.org/10.1111/j.1469-8137.2004.01154.x

Bragazza L, Lacumin P, Gerdol R (2010) Seasonal variation in nitrogen isotopic composition of bog plant litter during 3 years of field decomposition. Biol Fertil Soils 46:877–881. https://doi.org/10.1007/s00374-010-0483-7

Bünemann E, Oberson A, Frossard E (2011) Phosphorus in action: biological processes in soil phosphorus cycling. Springer, Berlin

Burt T, Holden J (2010) Changing temperature and rainfall gradients in the British uplands. Clim Res 45:57–70. https://doi.org/10.3354/cr00910

Cao X, Li H, Zhou Y, Song C (2020) The shift of mutualistic relationships among algae, free-living and attached bacteria through different nutrient addition mode: a mesocosm study. J Freshw Ecol 35:535–548. https://doi.org/10.1080/02705060.2020.1858984

Cape JN, Smith RI, Fowler D, Beswick K, Choularton T (2015) Long-term trends in rain and cloud chemistry in a region of complex topography. Atmos Res 153:335–347. https://doi.org/10.1016/j.atmosres.2014.09.003

Chen J, van Groenigen KJ, Hungate BA, Terrer C, van Groenigen JW, Maestre FT, Ying SC, Luo Y, Jorgensen U, Sinsabaugh RL, Olesen JE, Elsgaard L (2020) Long-term nitrogen loading alleviates phosphorus limitation in terrestrial ecosystems. Glob Change Biol 26(9):5077–5086. https://doi.org/10.1111/gcb.15218

Chiwa M, Sheppard LJ, Leith ID, Leeson SR, Tang YS, Cape JN (2018) Long-term interactive effects of N addition with P and K availability on N status of *Sphagnum*. Environ Pollut 237:468–472. https://doi.org/10.1016/j.envpol.2018.02.076

Comas X, Slater L (2004) Low-frequency electrical properties of peat. Water Resour Res 40:W12414. https://doi.org/10.1029/2004WR003534

Cui Y, Bing H, Fang L, Jiang M, Shen G, Yu J, Wang X, Zhu H, Wu Y, Zhang X (2021) Extracellular enzyme stoichiometry reveals the carbon and phosphorus limitations of microbial metabolisms in the rhizosphere and bulk soils in alpine ecosystems. Plant Soil 458:7–20. https://doi.org/10.1007/s11104-019-04159-x

Cui Y, Bing H, Moorhead DL, Delgado-Baquerizo M, Ye L, Yu J, Zhang S, Wang X, Peng S, Guo X, Zhu B, Chen J, Tan W, Wang Y, Zhang X, Fang L (2022) Ecoenzymatic stoichiometry reveals widespread soil phosphorus limitation to microbial metabolism across Chinese forests. Commun Earth Environ 3:184–191. https://doi.org/10.1038/s43247-022-00523-5

Cui Y, Peng S, Rillig MC, Camenzind T, Delgado-Baquerizo M, Terrer C, Xu X, Feng M, Wang M, Fang L, Zhu B, Du E, Moorhead DL, Sinsabaugh RL, Peñuelas J, Elser JJ (2025) Global patterns of nutrient limitation in soil microorganisms. PNAS 122(20):e2424552122. https://doi.org/10.1073/pnas.2424552122

Curtinrich HJ, Sebestyen SD, Griffiths NA, Hall SJ (2022) Warming stimulates iron-mediated carbon and nutrient cycling in mineral-poor peatlands. Ecosystems 25:44–60. https://doi.org/10.1007/s10021-021-00639-3

Drollinger S, Knorr KH, Knierzinger W, Glatzel S (2020) Peat decomposition proxies of Alpine bogs along a degradation gradient. Geoderma 369:114331–121143. https://doi.org/10.1016/j.geoderma.2020.114331

Dunn C, Jones TG, Girard A, Freeman C (2014) Methodologies for extracellular enzyme assays from wetland soils. Wetlands 34:9–17. https://doi.org/10.1007/s13157-013-0475-0

Elser JJ, Sterner RW, Gorokhova E, Fagan WF, Markow TA, Cotner JB, Harrison JF, Hobbie SE, Odell GM, Weider LW (2000) Biological stoichiometry from genes to ecosystems. Ecol Lett 3:540–550. https://doi.org/10.1111/j.1461-0248.2000.00185.x

Evans C, Morrison R, Burden A, Williamson J, Baird A, Brown E, Callaghan N, Chapman P, Cumming A, Dean H, Dixon S, Dooling G, Evans J, Gauci V, Grayson R, Haddaway N, He Y, Heppel K, Holden J, Worrall F (2016) Lowland peatland systems in England and Wales—evaluating greenhouse gas fluxes and carbon balances. Final report to Defra on project SP1210. Centre for Ecology and Hydrology, Bangor

Evans CD, Peacock M, Baird AJ, Artz RRE, Burden A, Callaghan N, Chapman PJ, Cooper HM, Coyle M, Craig E, Cumming A, Dixon S, Gauci V, Grayson RP, Helfter C, Heppell CM, Holden J, Jones DL, Kaduk J, Levy P, Matthews R, McNamara NP, Misselbrook T, Oakley S, Page SE, Rayment M, Ridley LM, Stanley KM, Williamson JL, Worrall F, Morrison R (2021) Overriding water-table control on managed peatland greenhouse gas emissions. Nature 593:548–552. https://doi.org/10.1038/s41586-021-03523-1

Feng X, Deventer MJ, Lonchar R, Ng GHC, Sebestyen SD, Griffis TJ, Millet DB, Kolka RK (2020) Climate sensitivity of peatland methane emissions mediated by seasonal hydrologic dynamics. Geophys Res Lett 47(17):e2020GL088875. https://doi.org/10.1029/2020GL088875

Fenner N, Freeman C (2011) Drought-induced carbon loss in peatlands. Nat Geosci 4:895–900. https://doi.org/10.1038/ngeo1323

Ferretto A, Brooker R, Aitkenhead M, Matthews R, Smith P (2019) Potential carbon loss from Scottish peatlands under climate change. Reg Environ Change 19:2101–2111. https://doi.org/10.1007/s10113-019-01550-3

Freeman C, Ostle N, Kang H (2001) An enzymic 'latch' on a global carbon store. Nature 409:149–150. https://doi.org/10.1038/35051650

Freeman C, Ostle NJ, Fenner N, Kang H (2004) A regulatory role for phenol oxidase during decomposition in peatlands. Soil Biol Biochem 36:1663–1667. https://doi.org/10.1016/j.soilbio.2004.07.012

Fülöp, O., Nunan, N., Gueye, M., & Jougnot, D. Electrical conductivity measurements as a proxy for diffusion-limited microbial activity in soils, *EGUsphere (preprint)*, https://doi.org/10.5194/egusphere-egu25-10876 (2025).

Gao S, Song Y, Song C, Wang X, Gong C, Ma X, Gao J, Cheng X, Du Y (2022) Long-term nitrogen addition alters peatland plant community structure and nutrient resorption efficiency. Sci Total Environ 844:157176. https://doi.org/10.1016/j.scitotenv.2022.157176

Gruber N, Deutsch C (2014) Redfield's evolving legacy. Nat Geosci 7:853–855. https://doi.org/10.1038/ngeo2308

Güsewell S, Koerselman W (2002) Variation in nitrogen and phosphorus concentrations of wetland plants. Perspect Plant Ecol Evol Syst 5:37–61. https://doi.org/10.1078/1433-8319-0000022

Güsewell S (2004) N:P ratios in terrestrial plants: variation and functional significance. New Phytol 164:243–266. https://doi.org/10.1111/j.1469-8137.2004.01192.x

Hollis D, Carlisle E, Kendon M, Packman S, Doherty A, Met Office (2025) HadUK-Grid Gridded Climate Observations on a 1km grid over the UK, v1.3.1.ceda (1836-2024), *NERC EDS Centre for Environmental Data Analysis*. https://doi.org/10.5285/f02cc6ddd92f45b18b9ab6ab544df7d9

IUSS Working Group WRB (2015) World reference base for soil resources 2014, update 2015: international soil classification system for naming soils and creating legends for soil maps. World Soil Resources Reports No. 106. FAO, Rome

Jayasekara C, Leigh C, Shimeta J, Silvester E, Grover S (2025) Organic matter decomposition in mountain peatlands: effects of substrate quality and peatland degradation. Plant Soil 506:639–654. https://doi.org/10.1007/s11104-024-06725-4

Jian S, Li J, Chen J, Wang G, Mayes MA, Dzantor KE, Hui D, Luo Y (2016) Soil extracellular enzyme activities, soil carbon and nitrogen storage under nitrogen fertilization: a meta-analysis. Soil Biol Biochem 101:32–43. https://doi.org/10.1016/j.soilbio.2016.07.003

Jiroušek M, Hájek M, Bragazza L (2011) Nutrient stoichiometry in *Sphagnum* along a nitrogen deposition gradient in highly polluted region of Central-East Europe. Environ Pollut 159:585–590. https://doi.org/10.1016/j.envpol.2010.10.004

Knorr KH, Horn MA, Borken W (2015) Significant nonsymbiotic nitrogen fixation in Patagonian ombrotrophic bogs. Glob Change Biol 21:2357–2365. https://doi.org/10.1111/gcb.12849

Koch O, Tscherko D, Kandeler E (2007) Temperature sensitivity of microbial respiration, nitrogen mineralization, and potential soil enzyme activities in organic alpine soils. Glob Biogeochem Cycles 21:GB4017. https://doi.org/10.1029/2007GB002983

Larmola T, Bubier JL, Kobyljanec C, Basiliko N, Juutinen S, Humphreys E, Preston M, Moore TR (2013) Vegetation feedbacks of nutrient addition lead to a weaker carbon sink in an ombrotrophic bog. Glob Chang Biol 19:3729–3739. https://doi.org/10.1111/gcb.12328

Limpens J, Berendse F, Klees H (2003) N deposition affects N availability in interstitial water, growth of *Sphagnum* and invasion of vascular plants in bog vegetation. New Phytol 157:339–347. https://doi.org/10.1046/j.1469-8137.2003.00667.x

Limpens J, Berendse F, Klees H (2004) How phosphorus availability affects the impact of nitrogen deposition on *Sphagnum* and vascular plants in bogs. Ecosystems 7:793–804. https://doi.org/10.1007/s10021-004-0274-9

Lindsay R (1995) Bogs: the ecology, classification and conservation of ombrotrophic mires. Scottish Natural Heritage, Edinburgh

Lindsay R, Charman DJ, Everingham F, O'Reilly RM, Palmer MA, Rowell TA, Stroud DA (1988) The Flow Country: the peatlands of Caithness and Sutherland. Joint Nature Conservation Committee, Peterborough

Lopes AAC, de Sousa DMG, Chaer GM, Junior FBR, Goedert WJ, Mendes IC (2015) Air-drying and long-term storage effects on β-glucosidase, acid phosphatase and arylsulfatase activities in a tropical savannah Oxisol. Appl Soil Ecol 93:68–77. https://doi.org/10.1016/j.apsoil.2015.04.001

Lunt PH, Fyfe RM, Tappin AD (2019) Role of recent climate change on carbon sequestration in peatland systems. Sci Total Environ 667:345–358. https://doi.org/10.1016/j.scitotenv.2019.02.239

Luo L, Zhu L, Hong W, Gu J-D, Shi D, He Y, Xiao Y, Tian D, Zhang S, Deng S, Lan T, Deng O (2021) Microbial resource limitation and regulation of soil carbon cycle in Zoige Plateau peatland soils. Catena 205:105478. https://doi.org/10.1016/j.catena.2021.105478

Machmuller MB, Mohan JE, Minucci JM, Phillips CA, Wurzburger N (2016) Season, but not experimental warming, affects the activity and temperature sensitivity of extracellular enzymes. Biogeochemistry 131:255–265. https://doi.org/10.1007/s10533-016-0277-6

Margalef O, Sardans J, Fernández-Martínez M, Molowny-Horas R, Janssens IA, Ciais P, Goll D, Richter A, Obersteiner M, Asensio D, Peñuelas J (2017) Global patterns of phosphatase activity in natural soils. Sci Rep 7:1337. https://doi.org/10.1038/s41598-017-01418-8

Moore TR, Dalva M (2001) Some controls on the release of dissolved organic carbon by plant tissues and soils. Soil Sci 166(1):38–47

Moore TR, Bubier JL, Bledzki L (2007) Litter decomposition in temperate peatland ecosystems: the effect of substrate and site. Ecosystems 10:949–963. https://doi.org/10.1007/s10021-007-9064-5

Moore TR, Large D, Talbot J, Wang M, Riley JL (2018) The stoichiometry of carbon, hydrogen, and oxygen in peat. J Geophys Res Biogeosci 123:3101–3110. https://doi.org/10.1029/2018JG004574

Mooshammer M, Wanek W, Zechmeister-Boltenstern S, Richter A (2014) Adjustment of microbial nitrogen use efficiency to carbon:nitrogen imbalances regulates soil nitrogen cycling. Nat Commun 5:3694. https://doi.org/10.1038/ncomms4694

Mori T (2020) Does ecoenzymatic stoichiometry really determine microbial nutrient limitations? Soil Biol Biochem 146:107816. https://doi.org/10.1016/j.soilbio.2020.107816

Mori T, Aoyagi R, Kitayama K, Mo J (2021) Does the ratio of β-1,4-glucosidase to β-1,4-N-acetylglucosaminidase indicate the relative resource allocation of soil microbes to C and N acquisition? Soil Biol Biochem 160:108363. https://doi.org/10.1016/j.soilbio.2021.108363

Mori T, Rosinger C, Margenot AJ (2023) Enzymatic C:N:P stoichiometry: questionable assumptions and inconsistencies to infer soil microbial nutrient limitation. Geoderma 429:116242. https://doi.org/10.1016/j.geoderma.2022.116242

Morton PA, Heinemeyer A (2019) Bog breathing: the extent of peat shrinkage and expansion on blanket bogs in relation to water table, heather management and dominant vegetation and its implications for carbon stock assessments. Wetlands Ecol Manag 27(2):467–482. https://doi.org/10.1007/s11273-019-09672-5

Motasim AM, Samsuri AW, Nabayi A, Akter A, Haque MA, Sukor ASA, Adibah AM (2024) Urea application in soil: processes, losses, and alternatives—a review. Discov Agric 2:42. https://doi.org/10.1007/s44279-024-00060-z

Mozafari B, Bruen M, Donohue S, Renou-Wilson F, O'Loughlin F (2023) Peatland dynamics: a review of process-based models and approaches. Sci Total Environ 877:162890. https://doi.org/10.1016/j.scitotenv.2023.162890

Murphy J, Riley JP (1962) A modified single solution method for the determination of phosphate in natural waters. Anal Chim Acta 27:31–36. https://doi.org/10.1016/S0003-2670(00)88444-5

Nannipieri P, Giagnoni L, Landi L, Renella G (2011) Role of phosphatase enzymes in soil. In: Bünemann E, Oberson A, Frossard E (eds) Phosphorus in Action. Soil Biology, vol 26. Springer, Berlin. https://doi.org/10.1007/978-3-642-15271-9_9

NatureScot. Carbon and Peatland 2016 map, *NERC Environmental Information Data Centre / NatureScot*. https://doi.org/https://opendata.nature.scot/datasets/snh::carbon-and-peatland-2016-map (2016)

Natural England, RSPB (2015) Climate change adaptation manual: evidence to support nature conservation in a changing climate. Natural England. https://publications.naturalengland.org.uk/publication/5629923804839936

Natural England. Priority Habitats Inventory (England), *Department for Environment, Food & Rural Affairs (Defra)*. https://naturalengland-defra.opendata.arcgis.com/datasets/Defra::priority-habitats-inventory-england/about (2025).

Oksanen J, Blanchet FG, Friendly M, Kindt R, Legendre P, McGlinn D, Minchin PR, O'Hara RB, Simpson GL, Solymos P, Stevens MHH, Szoecs E, Wagner H (2022) vegan: community ecology package. R package version 2.6–4. https://CRAN.R-project.org/package=vegan

Olde Venterink H, Wassen MJ, Verkroost AWM, De Ruiter PC (2003) Species richness–productivity patterns differ between N-, P-, and K-limited wetlands. Ecology 84:2191–2199. https://doi.org/10.1890/01-0639

Osburn ED, Yang G, Rillig MC, Strickland MS (2023) Evaluating the role of bacterial diversity in supporting soil ecosystem functions under anthropogenic stress. ISME Commun 3(1):66. https://doi.org/10.1038/s43705-023-00273-1

Parvin S, Blagodatskaya E, Becker JN, Kuzyakov Y, Uddin S, Dorodnikov M (2018) Depth rather than microrelief controls microbial biomass and kinetics of C-, N-, P- and S-cycle enzymes in peatland. Geoderma 324:67–76. https://doi.org/10.1016/j.geoderma.2018.03.006

Pedersen TL (2022) ggforce: accelerating 'ggplot2'. R package version 0.4.1. https://CRAN.R-project.org/package=ggforce

Pinsonneault AJ, Moore TR, Roulet NT (2016) Temperature the dominant control on the enzyme-latch across a range of temperate peatland types. Soil Biol Biochem 97:121–130. https://doi.org/10.1016/j.soilbio.2016.03.006

Ponziani M, Slob EC, Vanhala H, Ngan-Tillard DJM (2012) Influence of physical and chemical properties on the low-frequency complex conductivity of peat. Near Surf Geophys 10:491–501. https://doi.org/10.3997/1873-0604.2011037

Prosser JI, Speir TW, Stott DE (2011) Soil oxidoreductases and FDA hydrolysis. Methods Enzymol 9:103–124. https://doi.org/10.2136/sssabookser9.c6

Ptacnik R, Andersen T, Tamminen T (2010) Performance of the Redfield ratio and a family of nutrient limitation indicators as thresholds for phytoplankton N vs. P limitation. Ecosystems 13:1201–1214. https://doi.org/10.1007/s10021-010-9380-z

Qin L, Tian W, Freeman C, Jia Z, Yin X, Gao C, Zou Y, Jiang M (2024) Changes in bacterial communities during rice cultivation remove phenolic constraints on peatland carbon preservation. ISME Commun 4:ycae022. https://doi.org/10.1093/ismeco/ycae022

R Core Team (2012) R: a language and environment for statistical computing. R Foundation for Statistical Computing, Vienna, Austria

Ritson JP, Lees KJ, Hill J, Gallego-Sala A, Bebber DP (2025) Climate change impacts on blanket peatland in Great Britain. J Appl Ecol 62:701–714. https://doi.org/10.1111/1365-2664.14864

Rosinger C, Rousk J, Sandén H (2019) Can enzymatic stoichiometry be used to determine growth-limiting nutrients for microorganisms? A critical assessment in two subtropical soils. Soil Biol Biochem 128:115–126. https://doi.org/10.1016/j.soilbio.2018.10.011

Rowland CS, Marston CG, O'Neil AW (2025) Land Cover Map 2024 (10 m classified pixels, GB). NERC EDS Environmental Information Data Centre. https://doi.org/10.5285/4dd9df19-8df5-41a0-9829-8f6114e28db1

Sanchez G (2013) PLS path modeling with R. Trowchez Editions. https://cran.r-project.org/package=plspm

Schillereff DN, Chiverrell RC, Sjöström JK, Kylander ME, Boyle JF, Davies JAC, Toberman H, Tipping E (2021) Phosphorus supply affects long-term carbon accumulation in mid-latitude ombrotrophic peatlands. Commun Earth Environ 2:241. https://doi.org/10.1038/s43247-021-00316-2

Schlesinger WH, Bernhardt ES (2020) The global cycles of nitrogen, phosphorus and potassium. Biogeochemistry. https://doi.org/10.1016/B978-0-12-814608-8.00012-8

Sinsabaugh RL, Moorhead DL (1994) Resource allocation to extracellular enzyme production: a model for nitrogen and phosphorus control of litter decomposition. Soil Biol Biochem 26(10):1305–1311. https://doi.org/10.1016/0038-0717(94)90211-9

Sinsabaugh RL, Hill BH, Follstad Shah JJ (2009) Ecoenzymatic stoichiometry of microbial organic nutrient acquisition in soil and sediment. Nature 462:795–798. https://doi.org/10.1038/nature08632

Song Y, Song C, Meng H, Swarzenski CM, Wang X, Tan W (2017) Nitrogen additions affect litter quality and soil biochemical properties in a peatland of Northeast China. Ecol Eng 100:175–185. https://doi.org/10.1016/j.ecoleng.2016.12.025

Steinweg JM, Kostka JE, Hanson PJ, Schadt CW (2018) Temperature sensitivity of extracellular enzymes differs with peat depth but not with season in an ombrotrophic bog. Soil Biol Biochem 125:244–250. https://doi.org/10.1016/j.soilbio.2018.07.001

Strickland MS, Rousk J (2010) Considering fungal:bacterial dominance in soils—methods, controls, and ecosystem implications. Soil Biol Biochem 42:1385–1395. https://doi.org/10.1016/j.soilbio.2010.05.007

Swinnen W, Broothaerts N, Verstraeten G (2019) Modelling long-term blanket peatland development in Eastern Scotland. Biogeosciences 16:3977–3996. https://doi.org/10.5194/bg-16-3977-2019

Tang Z, Chi Z, Jiang F, Zhao M, Fu S, Wei L, Feng Q, Wu Y, Xu N (2025) Mechanisms and implications of phosphate retention in soils: insights from batch adsorption experiments and geochemical modeling. Water 17:998. https://doi.org/10.3390/w17070998

Temmink RJM, Vroom RJE, Van Dijk G, Käärmelahti SA, Koks AHW, Joosten H, Krebs M, Gaudig G, Brust K, Lamers LPM, Smolders AJP, Fritz C (2023) Restoring organic matter, carbon and nutrient accumulation in degraded peatlands: 10 years *Sphagnum* paludiculture. Biogeochemistry 167:347–361. https://doi.org/10.1007/s10533-023-01065-4

Tfaily MM, Cooper WT, Kostka JE, Chanton PR, Schadt CW, Hanson PJ, Iversen CM (2014) Organic matter transformation in the peat profile: coupled carbon and nitrogen cycling. J Geophys Res Biogeosci 119:661–675. https://doi.org/10.1002/2013JG002492

UNEP (2022) Global Peatlands Assessment—the state of the world's peatlands: evidence for action toward the conservation, restoration, and sustainable management of peatlands. Summary for Policy Makers. Global Peatlands Initiative, United Nations Environment Programme, Nairobi. https://doi.org/10.59117/20.500.11822/41222

Urban NR, Verry ES, Eisenreich SJ (1995) Retention and mobility of cations in a small peatland: trends and mechanisms. Water Air Soil Pollut 79:201–224. https://doi.org/10.1007/BF01100438

Urbanová Z, Hájek T (2021) Revisiting the concept of 'enzymic latch' on carbon in peatlands. Sci Total Environ 779:146384. https://doi.org/10.1016/j.scitotenv.2021.146384

Van Den Elzen E, Kox MAR, Harpenslager SF, Hensgens G, Fritz C, Jetten MSM, Ettwig KF, Lamers LPM (2017) Symbiosis revisited: phosphorus and acid buffering stimulate N_2 fixation but not *Sphagnum* growth. Biogeosciences 14:1111–1122. https://doi.org/10.5194/bg-14-1111-2017

Vesala R, Kiheri H, Hobbie EA, Nijk VD, Dise N, Larmola T (2021) Atmospheric nitrogen enrichment changes nutrient stoichiometry and reduces fungal N supply to peatland ericoid mycorrhizal shrubs. Sci Total Environ 794:148737. https://doi.org/10.1016/j.scitotenv.2021.148737

Vile MA, Wieder RK, Živković T, Scott KD, Vitt DH, Hartsock JA, Iosue CL, Quinn JC, Petix M, Fillingim HM, Popma JMA, Dynarski KA, Jackman TR, Albright CM, Wykoff DD (2014) N_2-fixation by methanotrophs sustains carbon and nitrogen accumulation in pristine peatlands. Biogeochemistry 121:317–328. https://doi.org/10.1007/s10533-014-0019-6

Wallenstein MD, Burns RG (2011) Ecology of extracellular enzyme activities and organic matter degradation in soil: a complex community-driven process. Methods Enzymol 9:35–55. https://doi.org/10.1007/978-3-642-14225-3_3

Wang M, Moore TR (2014) Carbon, nitrogen, phosphorus, and potassium stoichiometry in an ombrotrophic peatland reflects plant functional type. Ecosystems 17:673–684. https://doi.org/10.1007/s10021-014-9752-x

Wang M, Moore TR, Talbot J, Riley JL (2015) The stoichiometry of carbon and nutrients in peat formation. Glob Biogeochem Cycles 29:113–121. https://doi.org/10.1002/2014GB005000

Weedon JT, Aerts R, Kowalchuk GA, Van Bodegom PM (2014) No effects of experimental warming but contrasting seasonal patterns for soil peptidase and glycosidase enzymes in a sub-arctic peat bog. Biogeochemistry 117:55–66. https://doi.org/10.1007/s10533-013-9870-0

Welsh Government. Peatlands of Wales map, *Welsh Government*, https://doi.org/https://datamap.gov.wales/maps/peatlands-of-wales-maps/ (2022).

Wickham H (2016) ggplot2: elegant graphics for data analysis. Springer-Verlag, New York

Wickham H, François R, Henry L, Müller K (2023) dplyr: a grammar of data manipulation. R package version 1.1.3. https://CRAN.R-project.org/package=dplyr

Wieder RK, Vitt DH, Vile MA, Graham JA, Hartsock JA, Popma JMA, Fillingim H, House M, Quinn JC, Scott KD, Petix M, McMillen KJ (2020) Experimental nitrogen addition alters structure and function of a boreal poor fen: implications for critical loads. Sci Total Environ 733:138619. https://doi.org/10.1016/j.scitotenv.2020.138619

Wood S (2000) mgcv: mixed GAM computation vehicle with automatic smoothness estimation. https://doi.org/10.32614/CRAN.package.mgcv

Worrall F, Moody CS, Clay GD, Burt TP, Rose R (2016) The total phosphorus budget of a peat-covered catchment. J Geophys Res Biogeosci 121:1814–1828. https://doi.org/10.1002/2016JG003375

Xiong JB, Mahmood Q (2010) Adsorptive removal of phosphate from aqueous media by peat. Desalination 259:59–64. https://doi.org/10.1016/j.desal.2010.04.035

Xu Z, Wang Y, Sun D, Li H, Dong Y, Wang Z, Wang S (2022) Soil nutrients and nutrient ratios influence the ratios of soil microbial biomass and metabolic nutrient limitations in mountain peatlands. Catena 218:106528. https://doi.org/10.1016/j.catena.2022.106528

Xu H, Wang M, You C, Tan B, Xu L, Li H, Zhang L, Wang L, Liu S, Hou G, Liu Y, Xu Z, Sardans J, Peñuelas J (2024) Warming effects on C:N:P stoichiometry and nutrient limitation in terrestrial ecosystems. Soil Tillage Res 235:105896. https://doi.org/10.1016/j.still.2023.105896

Yang W, Xiang W, Bao Z, Huang C, Ma M, Lu X, Yao L, Wang Y (2022) Phosphorus sorption capacity of various iron-organic matter associations in peat soils. Environ Sci Pollut Res 29:77580–77592. https://doi.org/10.1007/s11356-022-21303-w

Yin T, Feng M, Qiu C, Peng S (2022) Biological nitrogen fixation and nitrogen accumulation in peatlands. Front Earth Sci 10:670867. https://doi.org/10.3389/feart.2022.670867

Zak D, Gelbrecht J, Steinberg CEW (2004) Phosphorus retention at the redox interface of peatlands adjacent to surface waters in Northeast Germany. Biogeochemistry 70:357–368. https://doi.org/10.1007/s10533-003-0895-7

Zeh LMT, Schellekens J, Limpens J, Bragazza L, Kalbitz K (2020) Vascular plants affect properties and decomposition of moss-dominated peat, particularly at elevated temperatures. Biogeosciences 17:4797–4813. https://doi.org/10.5194/bg-17-4797

Zhai Z, Lin L, Li T, Bu Z, Wang M (2025) Enzymatic stoichiometry and vector characteristics can indicate microbial resource limitation: empirical evidence from experiment with multiple nutrient addition. Ecosystems 28:4. https://doi.org/10.1007/s10021-024-00948-3

Zhang D, Wang L, Qin S, Kou D, Wang S, Zheng Z, Peñuelas J, Yang Y (2023) Microbial nitrogen and phosphorus co-limitation across permafrost region. Glob Chang Biol 29:3910–3923. https://doi.org/10.1111/gcb.16743

Zhao Y, Liu C, Li X, Ma L, Zhai G, Feng X (2023) *Sphagnum* increases soil's sequestration capacity of mineral-associated organic carbon via activating metal oxides. Nat Commun 14:5052. https://doi.org/10.1038/s41467-023-40863-0

Živković T, Helbig M, Moore TR (2022) Seasonal and spatial variability of biological N_2 fixation in a cool temperate bog. J Geophys Res Biogeosci 127(2):e2021JG006481. https://doi.org/10.1029/2021JG006481

Publisher's Note